NATIONAL ADVISORY COMMITTEE FOR AERONAUTICS

REPORT 1021

ANALYSIS OF PLANE-PLASTIC-STRESS PROBLEMS WITH AXIAL SYMMETRY IN STRAIN-HARDENING RANGE

By M. H. LEE WU

1951

For sale by the Superintendent of Documents, U. S. Government Printing Office, Washington 25, D. C. Yearly subscription, $4.00; foreign $5.25. Single copy price varies according to size - - - - - Price 25 cents

AERONAUTIC SYMBOLS

1. FUNDAMENTAL AND DERIVED UNITS

	Symbol	Metric		English	
		Unit	Abbreviation	Unit	Abbreviation
Length	l	meter	m	foot (or mile)	ft (or mi)
Time	t	second	s	second (or hour)	sec (or hr)
Force	F	weight of 1 kilogram	kg	weight of 1 pound	lb
Power	P	horsepower (metric)		horsepower	hp
Speed	V	kilometers per hour	kph	miles per hour	mph
		meters per second	mps	feet per second	fps

2. GENERAL SYMBOLS

W Weight$=mg$

g Standard acceleration of gravity$=9.80665$ m/s^2 or 32.1740 ft/sec^2

m Mass$=\frac{W}{g}$

I Moment of inertia$=mk^2$. (Indicate axis of radius of gyration k by proper subscript.)

μ Coefficient of viscosity

ν Kinematic viscosity

ρ Density (mass per unit volume)

Standard density of dry air, 0.12497 kg-m^{-4}-s^2 at 15° C and 760 mm; or 0.002378 lb-ft^{-4} sec^2

Specific weight of "standard" air, 1.2255 kg/m^3 or 0.07651 lb/cu ft

3. AERODYNAMIC SYMBOLS

S Area

S_w Area of wing

G Gap

b Span

c Chord

A Aspect ratio, $\frac{b^2}{S}$

V True air speed

q Dynamic pressure, $\frac{1}{2}\rho V^2$

L Lift, absolute coefficient $C_L=\frac{L}{qS}$

D Drag, absolute coefficient $C_D=\frac{D}{qS}$

D_0 Profile drag, absolute coefficient $C_{D_0}=\frac{D_0}{qS}$

D_i Induced drag, absolute coefficient $C_{D_i}=\frac{D_i}{qS}$

D_p Parasite drag, absolute coefficient $C_{D_p}=\frac{D_p}{qS}$

C Cross-wind force, absolute coefficient $C_C=\frac{C}{qS}$

i_w Angle of setting of wings (relative to thrust line)

i_t Angle of stabilizer setting (relative to thrust line)

Q Resultant moment

Ω Resultant angular velocity

R Reynolds number, $\rho\frac{Vl}{\mu}$ where l is a linear dimension (e.g., for an airfoil of 1.0 ft chord, 100 mph, standard pressure at 15° C, the corresponding Reynolds number is 935,400; or for an airfoil of 1.0 m chord, 100 mps, the corresponding Reynolds number is 6,865,000)

α Angle of attack

ϵ Angle of downwash

α_0 Angle of attack, infinite aspect ratio

α_i Angle of attack, induced

α_a Angle of attack, absolute (measured from zero-lift position)

γ Flight-path angle

REPORT 1021

ANALYSIS OF PLANE-PLASTIC-STRESS PROBLEMS WITH AXIAL SYMMETRY IN STRAIN-HARDENING RANGE

By M. H. LEE WU

Lewis Flight Propulsion Laboratory
Cleveland, Ohio

National Advisory Committee for Aeronautics

Headquarters, 1724 F Street NW., Washington 25, D. C.

Created by act of Congress approved March 3, 1915, for the supervision and direction of the scientific study of the problems of flight (U. S. Code, title 50, sec. 151). Its membership was increased from 12 to 15 by act approved March 2, 1929, and to 17 by act approved May 25, 1948. The members are appointed by the President, and serve as such without compensation.

TECHNICAL COMMITTEES

AERODYNAMICS
POWER PLANTS FOR AIRCRAFT
AIRCRAFT CONSTRUCTION
OPERATING PROBLEMS
INDUSTRY CONSULTING

Coordination of Research Needs of Military and Civil Aviation
Preparation of Research Programs
Allocation of Problems
Prevention of Duplication
Consideration of Inventions

LANGLEY AERONAUTICAL LABORATORY, Langley Field, Va.

LEWIS FLIGHT PROPULSION LABORATORY, Cleveland Airport, Cleveland, Ohio

AMES AERONAUTICAL LABORATORY, Moffett Field, Calif.

Conduct, under unified control, for all agencies, of scientific research on the fundamental problems of flight

---

OFFICE OF AERONAUTICAL INTELLIGENCE,
Washington, D. C.

Collection, classification, compilation, and dissemination of scientific and technical information on aeronautics

ERRATA

NACA Report 1021

ANALYSIS OF PLANE-PLASTIC-STRESS PROBLEMS
WITH AXIAL SYMMETRY IN STRAIN-HARDENING RANGE
By M. H. Lee Wu

Page 13, column 2: Line 16 should read "deformation the stress-(tangential stress) concentration . . . ."

NACA-Langley - 2-5-52 -1550

REPORT 1021

ANALYSIS OF PLANE-PLASTIC-STRESS PROBLEMS WITH AXIAL SYMMETRY IN STRAIN-HARDENING RANGE[1]

By M. H. Lee Wu

SUMMARY

A simple method is developed for solving plane-plastic-stress problems with axial symmetry in the strain-hardening range which is based on the deformation theory of plasticity employing the finite-strain concept. The equations defining the problems are first reduced to two simultaneous nonlinear differential equations involving two dependent variables: (a) the octahedral shear strain, and (b) a parameter indicating the ratio of principal stresses. By multiplying the load and dividing the radius by an arbitrary constant, it is possible to solve these problems without iteration for any value of the modified load. The constant is determined by the boundary condition.

This method is applied to a circular membrane under pressure, a rotating disk without and with a central hole, and an infinite plate with a circular hole. Two materials, Inconel X and 16–25–6, the octahedral shear stress-strain relations of which do not follow the power law, are used. Distributions of octahedral shear strain, as well as of principal stresses and strains, are obtained. These results are compared with the results of the same problems in the elastic range. The variation of load with maximum octahedral shear strain of the member is also investigated.

The following conclusions can be drawn:

1. Inasmuch as the ratios of the principal stresses remain essentially constant during loading for the materials considered, the deformation theory is applicable to this group of problems.

2. In plastic deformation, the distributions of the principal strains and of the octahedral shear strain are less uniform than in the elastic range, although the distributions of the principal stresses were more uniform. The stress-concentration factor around the hole is reduced with plastic deformation, but a high strain-concentration factor occurs.

3. For the rotating disk and the infinite plate the deformation that can be sustained by the member before failure depends mainly on the maximum octahedral shear strain of the material.

4. The added load that the member could sustain between the onset of yielding and failure depended mainly on the octahedral shear stress-strain relations of the material.

INTRODUCTION

In the design of turbine rotors, it is desirable to know the detailed stress and strain distributions in the strain-hardening range and the increase in load that can be sustained between the onset of yielding and failure. It is also desirable to know the effects of a notch or a hole in a turbine rotor or other machine members that are stressed in the strain-hardening range. If a member is thin, it can be analyzed on the basis of plane stress. For problems of this type for ideally plastic material, Nadai obtained solutions for a thin plate with a hole and a flat ring radially stressed (reference 1), and Nadai and Donnell obtained a solution for a rotating disk (reference 2). For materials having strain-hardening characteristics, a solution of plane-stress problems has been obtained by Gleyzal for a circular membrane under pressure (reference 3). The concept of infinitesimal strain was used and the solution was obtained by an iterative procedure with a good first approximate solution. The plastic laws were always satisfied by using a chart given in reference 3. In reference 4, a trial-and-error method is given for a rotating disk with very small plastic strain, in which the elastic stresses and strains are used as the first approximate values. An experimental investigation of high-speed rotating disks is given in reference 5; distributions of plastic strains (logarithmic strains) for different types of disk are measured. Reference 6 gives an experimental investigation of the burst characteristics of rotating disks; stress at the center of the disk is calculated by assuming that the material behaves elastically at the burst speed; the average tangential stress along the radius at burst speed is also calculated.

A simple method of solving plane-plastic-stress problems with axial symmetry in the strain-hardening range for finite strains was developed at the NACA Lewis laboratory during 1949–50. This method is based on the deformation theory of Hencky and Nadai (references 7 to 9), which is derived for the condition of constant directions and ratios of the principal stresses during loading. The equations of equilibrium, strain, and plastic law are reduced to two simultaneous nonlinear differential equations involving three variables, one independent and two dependent, that can be integrated numerically to any desired accuracy. These variables are the proportionate radial distance, the octahedral shear strain, and a parameter α that indicates the ratio of principal stresses. The magnitude of variation in calculated values of the parameter α with change in load directly indicates whether the deformation theory is applicable to the problem.

[1] Supersedes NACA TN 2217, "Analysis of Plane-Stress Problems With Axial Symmetry in Strain-Hardening Range" by M. H. Lee Wu, 1950.

The method developed is applied to: (1) a circular membrane under pressure, in order to compare results obtained by this method with those obtained by Gleyzal (reference 3); (2) rotating disks without and with a circular central hole, in order to investigate plastic deformation in such disks and the effects of the hole; and (3) an infinite plate with a circular hole or a flat ring radially stressed, in order to investigate the effects of the hole in the strain-hardening range.

In the investigation of (2) and (3), two materials, Inconel X and 16–25–6, with different strain-hardening characteristics were used in order to determine the effect of the octahedral shear stress-strain curve on plastic deformation. The octahedral shear stress of these two materials is not a power function of the octahedral shear strain, so that more general information can be obtained. Distributions of stresses and strains of the same problems in the elastic range are also calculated for purposes of comparison.

Acknowledgment is made to Professor D. C. Drucker for his discussion of this work and for his suggestion to examine whether the logarithmic strain could be applied correctly to the present problems and his suggestion to plot the stress-strain curves of Inconel X and 16–25–6 on a logarithmic scale in order to show that these materials do not obey the power law.

SYMBOLS

The following symbols are used in this report:

A, B, C, D, E, F	coefficients of nonlinear differential equations; functions of α, γ, and $\frac{r}{k}$
a	initial radius of hole
b	initial outside radius of membrane, rotating disk, or flat ring
c	initial outside radius of plate, very large compared with radius a
G, H, J, L	trigonometric functions of α
h	instantaneous thickness of membrane, rotating disk, or plate
h_{init}	initial thickness of membrane, disk, or plate
K_1, K_2	arbitrary loading constants
k	constant having a dimension of length
p	pressure on membrane
r	radial coordinate of undeformed membrane, disk, or plate
s	arc length
u	radial displacement
w	axial displacement
z	axial coordinate
α	parameter indicating ratio of principal stresses
γ	octahedral shear strain
ϵ	logarithmic strain (natural strain), logarithm of instantaneous length divided by initial length of element
θ	angular coordinate
ρ	mass per unit volume
σ	true normal stress, normal force per unit instantaneous area
τ	octahedral shear stress
ω	angular velocity
Subscripts:	
b	at radius b
c	at radius c
o	at center for member without hole; at radius a for member with concentric circular hole
1, 2, 3	principal directions in general
r, θ, z	principal directions: radial, tangential, and axial directions

STRESS-STRAIN RELATIONS IN PLASTIC DEFORMATION

The deformation theory of plasticity for ideally plastic materials was developed by Hencky from the theory of Saint Venant-Levy-Mises for the cases in which the directions and the ratios of principal stresses remain constant during loading (reference 7). Nadai extended the theory to include materials having strain-hardening characteristics (references 8 and 9). The conditions for the deformation theory have been emphasized by Nadai (reference 9, p. 209), Ilyushin (references 10 and 11), Prager (reference 12), and Drucker (reference 13). Experiments conducted by Davis (reference 14), Osgood (reference 15), and others on thin tubes subjected to combined loads with the directions and the ratios of the principal stresses constant throughout the tube and remaining constant during loading show that good results can be expected from the deformation theory.

In more recent experiments on thin tubes by Fraenkel (reference 16) and Davis and Parker (reference 17), it has been shown that even with considerable variation of the ratios of principal stresses during loading the strains obtained from the experiments were in good agreement with the strains predicted by use of the deformation theory. Further experimental investigation is needed to determine the extent to which the variation of ratios of principal stresses is permissible with the deformation theory. However, when the variation is small (approximately 10 percent over the strain-hardening range), the deformation theory can be expected to give good results.

In the present problems with axial symmetry, the directions of the axes of the principal stresses remain fixed during loading and it is probable that the ratios of principal strains and of principal stresses also remain approximately constant. The deformation theory previously discussed is therefore used. The stress-strain relations are as follows:

$$\epsilon_1+\epsilon_2+\epsilon_3=0 \tag{1}$$

$$\frac{\sigma_1-\sigma_2}{\epsilon_1-\epsilon_2}=\frac{\sigma_2-\sigma_3}{\epsilon_2-\epsilon_3}=\frac{\sigma_3-\sigma_1}{\epsilon_3-\epsilon_1} \tag{2}$$

$$\tau=\tau(\gamma) \tag{3}$$

where

$$\tau=\frac{1}{3}[(\sigma_1-\sigma_2)^2+(\sigma_2-\sigma_3)^2+(\sigma_3-\sigma_1)^2]^{1/2} \tag{4a}$$

$$\gamma=\frac{2}{3}[(\epsilon_1-\epsilon_2)^2+(\epsilon_2-\epsilon_3)^2+(\epsilon_3-\epsilon_1)^2]^{1/2} \tag{4b}$$

From equations (1), (2), and (4a) or (4b), the following relations are obtained:

$$\epsilon_1=\frac{1}{3}\frac{\gamma}{\tau}\left[\sigma_1-\frac{1}{2}(\sigma_2+\sigma_3)\right]$$

$$\epsilon_2=\frac{1}{3}\frac{\gamma}{\tau}\left[\sigma_2-\frac{1}{2}(\sigma_3+\sigma_1)\right]$$

$$\epsilon_3=\frac{1}{3}\frac{\gamma}{\tau}\left[\sigma_3-\frac{1}{2}(\sigma_1+\sigma_2)\right]$$

For plane-stress problems $\sigma_3=0$. It is convenient to use cylindrical coordinates for the problems considered; the principal directions 1, 2, and 3 in the preceding equations become radial, circumferential, and axial directions, respectively. The equations thus become

$$\epsilon_r+\epsilon_\theta+\epsilon_z=0 \tag{1a}$$

$$\tau=\frac{\sqrt{2}}{3}(\sigma_r^2-\sigma_r\sigma_\theta+\sigma_\theta^2)^{1/2} \tag{5a}$$

$$\gamma=2\sqrt{\frac{2}{3}}(\epsilon_r^2+\epsilon_r\epsilon_\theta+\epsilon_\theta^2)^{1/2} \tag{5b}$$

and

$$\epsilon_r=\frac{1}{3}\frac{\gamma}{\tau}\left(\sigma_r-\frac{1}{2}\sigma_\theta\right) \tag{6a}$$

$$\epsilon_\theta=\frac{1}{3}\frac{\gamma}{\tau}\left(\sigma_\theta-\frac{1}{2}\sigma_r\right) \tag{6b}$$

$$\epsilon_z=\frac{1}{3}\frac{\gamma}{\tau}\left[-\frac{1}{2}(\sigma_r+\sigma_\theta)\right]=-(\epsilon_r+\epsilon_\theta) \tag{6c}$$

When σ_r and σ_θ are expressed in terms of ϵ_r and ϵ_θ, there is obtained

$$\left.\begin{aligned}\sigma_r&=2\frac{\tau}{\gamma}(2\epsilon_r+\epsilon_\theta)\\ \sigma_\theta&=2\frac{\tau}{\gamma}(2\epsilon_\theta+\epsilon_r)\end{aligned}\right\} \tag{7}$$

Because large deformations in the strain-hardening range will be considered, the concept that the change of dimension of an element is infinitesimal compared with the original dimension of the element is not accurate enough. Hence, the finite-strain concept, which considers the instantaneous dimension of the element, is used. (The equations of infinitesimal strains considered as special cases of finite strains are given in appendix A.) The stress is then equal to the force divided by the instantaneous area and the strains are defined by the following equation:

$$\delta(\epsilon_j)=\frac{\delta(l_j)}{l_j}$$

where l_j is the instantaneous length of a small element having the original length of $(l_j)_0$ and j is any principal direction. During plastic deformation, the plastic strains at a particular state depend on the path by which that state is reached. For the paths along which the ratios of principal stresses remain constant during loading, however, the octahedral shear stress-strain relation, the value of the octahedral shear strain, and the values of the principal strains are defined by the initial and final states (references 14, 15, and reference 9, p. 209); $\delta(\epsilon_j)$ is then an exact differential and

$$\epsilon_j=\log_e\frac{l_j}{(l_j)_0} \text{ or } e^{\epsilon_j}=\frac{l_j}{(l_j)_0} \tag{8}$$

It should be noted that the condition under which equation (8) was obtained is also one of the conditions under which the deformation theory is derived; as long as the deformation theory is applicable, equation (8) can also be used.

EQUATIONS OF EQUILIBRIUM AND STRAINS INVOLVING DISPLACEMENTS

CIRCULAR MEMBRANE UNDER PRESSURE

Equations of equilibrium and equations of strain are derived for a circular membrane under pressure. The membrane considered is so thin that bending stress can be neglected (reference 18, p. 576). Figure 1 shows the membrane clamped at the rim and subjected to a pressure p and

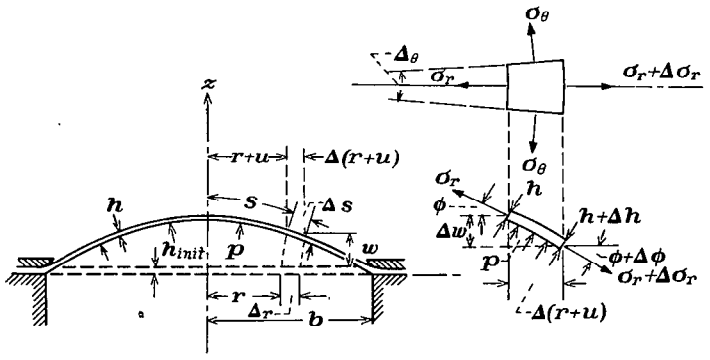

FIGURE 1.—Thin circular membrane (under pressure) and its element in deformed state.

a small element defined by $\Delta\theta$ and Δs taken at radius $r+u$ in the deformed state. In the undeformed state, the same element would be at radius r and defined by $\Delta\theta$ and Δr. The dotted lines represent an undeformed membrane. The instantaneous thickness of the element and the stresses acting on the element are also shown in the figure. Two principal stresses are σ_r and σ_θ, and φ is the angle between σ_r and the original radial direction.

Equations of equilibrium.—When all the forces acting on the element in the direction of σ_r are summed up, the following equation of equilibrium is obtained:

$$\sigma_r(r+u)h\Delta\theta-(\sigma_r+\Delta\sigma_r)[r+u+\Delta(r+u)]\Delta\theta(h+\Delta h)\cos\Delta\varphi+$$
$$2\sigma_\theta\Delta s\left(h+\frac{1}{2}\Delta h\right)\sin\frac{\Delta\theta}{2}\cos\varphi-p\Delta s(r+u)\Delta\theta\sin\frac{\Delta\varphi}{2}=0$$

When $\Delta(r+u)$ approaches zero as a limit, the differential equation of equilibrium may be obtained:

$$(r+u)\frac{d(\sigma_r h)}{d(r+u)}=h(\sigma_\theta-\sigma_r) \tag{9}$$

A cap of the membrane bounded by radius $r+u$ and the forces acting on it are shown in figure 2. Summing up the forces in the z-direction yields

$$p\pi(r+u)^2=\sigma_r\frac{dw}{ds}2\pi h(r+u)$$

or

$$\left[\frac{dw}{d(r+u)}\right]^2=\frac{1}{\left[\frac{2h\sigma_r}{p(r+u)}\right]^2-1} \tag{10}$$

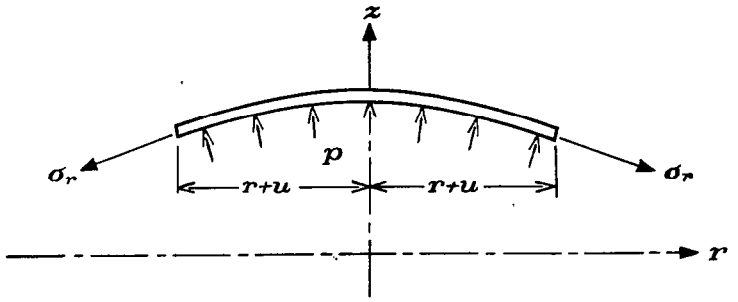

FIGURE 2.—Cap of membrane with radius $r+u$ in deformed state.

Equations of strains.—Inasmuch as the element at radius r, defined by $\Delta\theta$ and Δr in the undeformed state, is moved by the application of pressure p (fig. 1) to radius $r+u$ and defined by $\Delta\theta$ and Δs, by use of equation (8) the strains are

$$\epsilon_r=\log_e\frac{ds}{dr}$$
$$\epsilon_\theta=\log_e\frac{r+u}{r}$$
$$\epsilon_z=\log_e\frac{h}{h_{init}}$$

Then

$$e^{\epsilon_r}=\frac{d(r+u)}{dr}\left\{1+\left[\frac{dw}{d(r+u)}\right]^2\right\}^{1/2} \tag{11a}$$
$$e^{\epsilon_\theta}=\frac{r+u}{r} \tag{11b}$$
$$e^{\epsilon_z}=\frac{h}{h_{init}} \tag{11c}$$

ROTATING DISK

Equation of equilibrium.—A disk of radius b and thickness h, rotating about its axis with angular speed ω, and an element taken at radius $r+u$, defined by $\Delta\theta$ and $\Delta(r+u)$, are shown in figure 3 with all the external forces acting on the element.

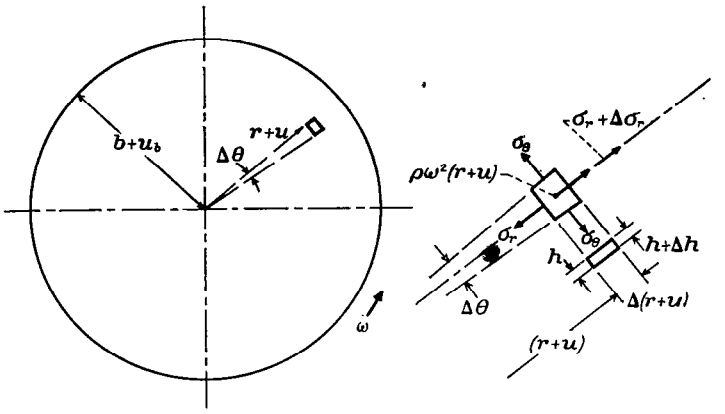

FIGURE 3.—Rotating disk and its element.

Summing up all forces acting on the element in the radial direction yields

$$\sigma_r(r+u)h\Delta\theta-(\sigma_r+\Delta\sigma_r)[r+u+\Delta(r+u)]\Delta\theta(h+\Delta h)+$$
$$2\sigma_\theta[\Delta(r+u)]\left(h+\frac{1}{2}\Delta h\right)\sin\frac{\Delta\theta}{2}-$$
$$\omega^2\left[r+u+\frac{1}{2}\Delta(r+u)\right]\frac{\rho\pi[(r+\Delta r)^2-r^2]\Delta\theta}{2\pi}h_{init}=0$$

When $\Delta(r+u)$ approaches zero as a limit, the following equation of equilibrium is obtained:

$$(r+u)\frac{d(\sigma_r h)}{d(r+u)}=(\sigma_\theta-\sigma_r)h-\rho\omega^2r^2h_{init}\frac{r+u}{r}\frac{dr}{d(r+u)} \tag{12}$$

Equations of strains.—The strains are

$$e^{\epsilon_r}=\frac{d(r+u)}{dr} \tag{13a}$$
$$e^{\epsilon_\theta}=\frac{r+u}{r} \tag{13b}$$
$$e^{\epsilon_z}=\frac{h}{h_{init}} \tag{13c}$$

INFINITE PLATE WITH CIRCULAR HOLE OR FLAT RING RADIALLY STRESSED

An infinite plate uniformly stressed in its plane in all directions and having a circular hole is shown in figure 4. The whole system is equivalent to a very large circular plate of radius c with a small concentric circular hole radially subjected to the same uniform stress σ on the outer boundary. The solution obtained for such a plate within any radius b can also be considered as a solution of a flat ring with outer radius b and inner radius a, that is, uniformly loaded at the outer boundary with the radial stress σ_b obtained in the plate solution.

The equations for this case can be obtained in a manner similar to the two previous cases, or by simply setting dw/dr and w equal to zero in equations for the membrane, or by setting ω equal to zero in the equation for the rotating disk.

EQUATIONS OF EQUILIBRIUM AND COMPATIBILITY IN TERMS OF PRINCIPAL STRESSES AND STRAINS

CIRCULAR MEMBRANE UNDER PRESSURE

A set of ten independent equations (equations (1a), (3), (5b), (6a), (6b), (9), (10), (11a), (11b), and (11c)) involving the ten unknowns σ_r, σ_θ, ϵ_r, ϵ_θ, ϵ_z, γ, τ, h, u, and w define the problem of the circular membrane under pressure. If equation (11b) is differentiated with respect to r and combined with equation (11a),

$$r\frac{d\epsilon_\theta}{dr}=\frac{e^{(\epsilon_r-\epsilon_\theta)}}{\left\{1+\left[\frac{dw}{d(r+u)}\right]^2\right\}^{1/2}}-1 \tag{14}$$

Substituting equation (10) in equation (14) to eliminate w yields the following equation of compatibility:

$$r\frac{d\epsilon_\theta}{dr}=e^{(\epsilon_r-\epsilon_\theta)}\left\{1-\left[\frac{p(r+u)}{2h\sigma_r}\right]^2\right\}^{1/2}-1 \tag{15}$$

Equations (9) and (15) can be simplified by using equations (11) to eliminate u and h, which results in

$$r\frac{d\sigma_r}{dr}+\sigma_r r\frac{d\epsilon_z}{dr}=(\sigma_\theta-\sigma_r)e^{(\epsilon_r-\epsilon_\theta)}\left\{1-\left[\frac{rpe^{(\epsilon_\theta-\epsilon_z)}}{2h_{init}\sigma_r}\right]^2\right\}^{1/2} \tag{16}$$

and

$$r\frac{d\epsilon_\theta}{dr}=e^{(\epsilon_r-\epsilon_\theta)}\left\{1-\left[\frac{rpe^{(\epsilon_\theta-\epsilon_z)}}{2h_{init}\sigma_r}\right]^2\right\}^{1/2}-1 \tag{17}$$

The ten equations defining this problem are now reduced to seven independent equations, (1a), (6a), (6b), (5b), (3), (16), and (17), with the seven unknowns σ_r, σ_θ, ϵ_r, ϵ_θ, ϵ_z, τ, and γ.

The solution of the problem is simplified by introducing an arbitrary constant k into equations (16) and (17):

$$\left.\begin{aligned}\frac{r}{k}\frac{d\sigma_r}{d\left(\frac{r}{k}\right)}+\sigma_r\frac{r}{k}\frac{d\epsilon_z}{d\left(\frac{r}{k}\right)}&=(\sigma_\theta-\sigma_r)e^{(\epsilon_r-\epsilon_\theta)}\left\{1-\left[\frac{pk}{h_{init}}\frac{r}{k}\frac{e^{(\epsilon_\theta-\epsilon_z)}}{2\sigma_r}\right]^2\right\}^{1/2}\\ \frac{r}{k}\frac{d\epsilon_\theta}{d\left(\frac{r}{k}\right)}&=e^{(\epsilon_r-\epsilon_\theta)}\left\{1-\left[\frac{pk}{h_{init}}\frac{r}{k}\frac{e^{(\epsilon_\theta-\epsilon_z)}}{2\sigma_r}\right]^2\right\}^{1/2}-1\end{aligned}\right\} \tag{18}$$

where k is any arbitrary unknown constant with the dimension of length. By use of the two parameters r/k and pk/h_{init}, it is possible to solve the problem in a simple, direct way without the use of the iteration. This will be further discussed in the section "Methods of Numerical Integration."

ROTATING DISK

For the rotating disk there are nine independent relations (equations (1a), (3), (5b), (6a), (6b), (12), (13a), (13b), and (13c)) with the nine unknowns σ_r, σ_θ, ϵ_r, ϵ_θ, ϵ_z, γ, τ, h, and u. If equation (13b) is differentiated with respect to r and combined with equation (13a), the following compatibility equation is obtained:

$$r\frac{d\epsilon_\theta}{dr}=e^{(\epsilon_r-\epsilon_\theta)}-1 \tag{19}$$

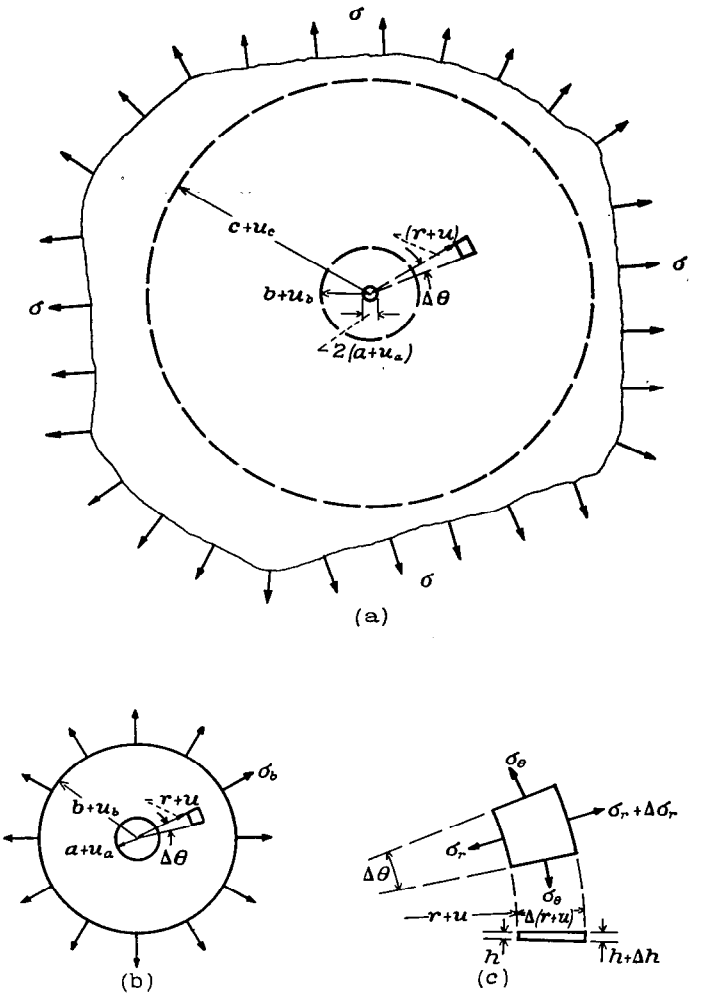

(a) Infinite plate with circular hole uniformly stressed in its plane in all directions.
(b) Flat ring radially stressed.
(c) Element.

FIGURE 4.—Infinite plate with circular hole, flat ring radially stressed, and its element in deformed state.

As in the case of the membrane, u and h can be eliminated from the equilibrium equation (12) by using equations (13), which yields

$$r\frac{d\sigma_r}{dr}+\sigma_r r\frac{d\epsilon_z}{dr}=(\sigma_\theta-\sigma_r)e^{(\epsilon_r-\epsilon_\theta)}-\rho\omega^2r^2e^{(-\epsilon_z)} \tag{20}$$

The nine equations defining this problem are now reduced to seven independent equations, (1a), (6a), (6b), (5b), (3), (19), and (20), with the seven unknowns σ_r, σ_θ, ϵ_r, ϵ_θ, ϵ_z, τ, and γ.

The solution of the problem is made simpler by introducing an arbitrary constant k into equations (19) and (20):

$$\left.\begin{aligned}\frac{r}{k}\frac{d\sigma_r}{d\left(\frac{r}{k}\right)}+\sigma_r\frac{r}{k}\frac{d\epsilon_z}{d\left(\frac{r}{k}\right)}&=(\sigma_\theta-\sigma_r)e^{(\epsilon_r-\epsilon_\theta)}-\rho(\omega k)^2\left(\frac{r}{k}\right)^2e^{(-\epsilon_z)}\\ \frac{r}{k}\frac{d\epsilon_\theta}{d\left(\frac{r}{k}\right)}&=e^{(\epsilon_r-\epsilon_\theta)}-1\end{aligned}\right\} \tag{21}$$

By use of the parameters r/k and ωk instead of r and ω, a simple direct solution is possible for any arbitrary value of ωk with k to be determined by the boundary condition.

INFINITE PLATE WITH CIRCULAR HOLE OR FLAT RING RADIALLY STRESSED

The equations of equilibrium and compatibility for the infinite plate with a circular hole or the flat ring radially stressed are:

$$\left.\begin{aligned} \frac{r}{a}\frac{d\sigma_r}{d\left(\frac{r}{a}\right)}+\sigma_r\frac{r}{a}\frac{d\epsilon_z}{d\left(\frac{r}{a}\right)}&=(\sigma_\theta-\sigma_r)\,e^{(\epsilon_r-\epsilon_\theta)} \\ \frac{r}{a}\frac{d\epsilon_\theta}{d\left(\frac{r}{a}\right)}&=e^{(\epsilon_r+\epsilon_\theta)}-1 \end{aligned}\right\} \tag{22}$$

The problem is defined by equations (22) together with equations (1a), (6a), (6b), (5b), and (3) (seven equations with seven unknowns).

EQUATIONS OF EQUILIBRIUM AND COMPATIBILITY IN TERMS OF OCTAHEDRAL SHEAR STRAIN AND PARAMETER INDICATING RATIO OF PRINCIPAL STRESSES

In the preceding section, displacements are eliminated from the equations, which result in seven equations involving the seven unknown quantities σ_r, σ_θ, ϵ_r, ϵ_θ, ϵ_z, τ, and γ. The quantity ϵ_z can be expressed in terms of ϵ_r and ϵ_θ (from equation (1a)). Two of the four unknowns σ_r, σ_θ, ϵ_r, and ϵ_θ can be eliminated by using equations (6a) and (6b) or (7). The quantity τ is a known function of γ that is experimentally determined. The problem is then reduced to one involving three unknowns. Obtaining the solution of the resulting equations is not, however, a simple matter; the iterative process is usually needed.

It is proposed that this can be avoided by using the following transformation:

$$\sigma_\theta+\sigma_r=3\sqrt{2}\tau\sin\alpha$$

$$\sigma_\theta+\sigma_r=\sqrt{6}\tau\cos\alpha$$

or

$$\left.\begin{aligned} \sigma_r&=\sqrt{\frac{3}{2}}\tau(\sqrt{3}\sin\alpha-\cos\alpha) \\ \sigma_\theta&=\sqrt{\frac{3}{2}}\tau(\sqrt{3}\sin\alpha+\cos\alpha) \end{aligned}\right\} \tag{23}$$

Then σ_r and σ_θ satisfy equation (5a), because the yielding surfaces are ellipses according to the deformation theory. The octahedral shear stress τ, a function of γ, in the preceding equations varies with r/k and also with loading. Such a transformation has been used for ideally plastic material (τ=constant) by Nadai in the section "Yielding in Thin Plate With Circular Hole or Flat Rings Radially Stressed" (reference 1, p. 189) and for a rotating disk (reference 2). From equations (6a), (6b), and (23), the principal strains also can be expressed in terms of γ and α:

$$\left.\begin{aligned} \epsilon_r&=\frac{\gamma}{2\sqrt{2}}(\sin\alpha-\sqrt{3}\cos\alpha) \\ \epsilon_\theta&=\frac{\gamma}{2\sqrt{2}}(\sin\alpha+\sqrt{3}\cos\alpha) \end{aligned}\right\} \tag{24}$$

The equations of equilibrium and compatibility for the three problems considered herein are then obtained in terms of γ and α in the following form:

$$\left.\begin{aligned} A\frac{r}{k}\frac{d\alpha}{d\left(\frac{r}{k}\right)}+B\frac{r}{k}\frac{d\gamma}{d\left(\frac{r}{k}\right)}&=C \\ D\frac{r}{k}\frac{d\alpha}{d\left(\frac{r}{k}\right)}+E\frac{r}{k}\frac{d\gamma}{d\left(\frac{r}{k}\right)}&=F \end{aligned}\right\} \tag{25}$$

where the coefficients A, B, C, D, E, and F are functions of α, γ, and r/k. For the circular membrane under pressure, from equation (18),

$$\left.\begin{aligned} A&=(\sqrt{3}\cos\alpha+\sin\alpha)-(\sqrt{3}\sin\alpha-\cos\alpha)\frac{\gamma\cos\alpha}{\sqrt{2}} \\ B&=(\sqrt{3}\sin\alpha-\cos\alpha)\left(\frac{\gamma}{\tau}\frac{d\tau}{d\gamma}-\frac{\gamma\sin\alpha}{\sqrt{2}}\right)\frac{1}{\gamma} \\ C&=2(\cos\alpha)\,e^{\left(-\sqrt{\frac{3}{2}}\gamma\cos\alpha\right)} \\ &\qquad\left[1-\frac{e^{\sqrt{\frac{3}{2}}(\sqrt{3}\sin\alpha+\cos\alpha)\gamma}}{6\tau^2(\sqrt{3}\sin\alpha-\cos\alpha)^2}\left(\frac{r}{k}\right)^2\left(\frac{pk}{h_{init}}\right)^2\right]^{1/2} \\ D&=(\sqrt{3}\sin\alpha-\cos\alpha)\gamma \\ E&=-(\sqrt{3}\cos\alpha+\sin\alpha) \\ F&=2\sqrt{2} \\ &\left\{1-e^{\left(-\sqrt{\frac{3}{2}}\gamma\cos\alpha\right)}\left[1-\frac{e^{\sqrt{\frac{3}{2}}(\sqrt{3}\sin\alpha+\cos\alpha)\gamma}}{6\tau^2(\sqrt{3}\sin\alpha-\cos\alpha)^2}\left(\frac{r}{k}\right)^2\left(\frac{pk}{h_{init}}\right)^2\right]^{1/2}\right\} \end{aligned}\right\} \tag{26}$$

For the rotating disk, from equation (21),

$$\left.\begin{aligned} A&=(\sqrt{3}\cos\alpha+\sin\alpha)-(\sqrt{3}\sin\alpha-\cos\alpha)\frac{\gamma\cos\alpha}{\sqrt{2}} \\ B&=(\sqrt{3}\sin\alpha-\cos\alpha)\left(\frac{\gamma}{\tau}\frac{d\tau}{d\gamma}-\frac{\gamma\sin\alpha}{\sqrt{2}}\right)\frac{1}{\gamma} \\ C&=2(\cos\alpha)\,e^{\left(-\sqrt{\frac{3}{2}}\gamma\cos\alpha\right)}-\sqrt{\frac{2}{3}}\rho(\omega k)^2\frac{1}{\tau}\left(\frac{r}{k}\right)^2 e^{\frac{\gamma}{\sqrt{2}}\sin\alpha} \\ D&=(\sqrt{3}\sin\alpha-\cos\alpha)\gamma \\ E&=-(\sqrt{3}\cos\alpha+\sin\alpha) \\ F&=2\sqrt{2}\left[1-e^{\left(-\sqrt{\frac{3}{2}}\gamma\cos\alpha\right)}\right] \end{aligned}\right\} \tag{27}$$

For the infinite plate with a circular hole, from equation (22),

$$\left.\begin{aligned} A&=(\sqrt{3}\cos\alpha+\sin\alpha)-(\sqrt{3}\sin\alpha-\cos\alpha)\frac{\gamma\cos\alpha}{\sqrt{2}}\\ B&=(\sqrt{3}\sin\alpha-\cos\alpha)\left(\frac{\gamma}{\tau}\frac{d\tau}{d\gamma}-\frac{\gamma\sin\alpha}{\sqrt{2}}\right)\frac{1}{\gamma}\\ C&=2(\cos\alpha)\,e^{\left(-\sqrt{\frac{3}{2}}\gamma\cos\alpha\right)}\\ D&=(\sqrt{3}\sin\alpha-\cos\alpha)\,\gamma\\ E&=-(\sqrt{3}\cos\alpha+\sin\alpha)\\ F&=2\sqrt{2}\left[1-e^{\left(-\sqrt{\frac{3}{2}}\gamma\cos\alpha\right)}\right] \end{aligned}\right\} \quad (28)$$

With these transformations, the solution of the problems is reduced to simply a numerical integration of the two simultaneous differential equations (equations (25)) involving the two unknowns γ and α. Furthermore, the parameter γ, being the octahedral shear strain, directly indicates the stage of plastic deformation at any point under any load. (In plastic problems, according to the deformation theory, the individual stress and strain distributions cannot give as clear a picture of the stage of plastic deformation as can the octahedral shear strain.) Also, the parameter α indicates the ratio of the principal stresses or strains. At any point, if α remains constant during loading, the ratio of principal stresses at that point remains fixed. The value of α obtained at each point in the calculation during loading directly indicates whether or not the deformation theory is applicable to the problem.

The value of α is known at the boundaries or the center. This value can be determined from equations (23) and (24). For the circular membrane under pressure,
when $r/b=0$,

$$\sigma_r=\sigma_\theta$$

$$\alpha=\frac{\pi}{2}=1.5708$$

when $r/b=1$,

$$\epsilon_\theta=0$$

$$\alpha=\frac{2}{3}\pi=2.0944$$

For the rotating disk without a hole,
when $r/b=0$,

$$\sigma_r=\sigma_\theta$$

$$\alpha=\frac{\pi}{2}=1.5708$$

when $r/b=1$,

$$\sigma_r=0$$

$$\alpha=\frac{\pi}{6}=0.5236$$

For the rotating disk with a hole,
when $r/a=1$ and $r/b=1$,

$$\sigma_r=0$$

$$\alpha=\frac{\pi}{6}=0.5236$$

For the infinite plate with a circular hole,
when $r/a=1$,

$$\sigma_r=0$$

$$\alpha=\frac{\pi}{6}=0.5236$$

when r/a approaches c/a or a value that is large compared with 1,

$$\sigma_r=\sigma_\theta$$

$$\alpha=\frac{\pi}{2}=1.5708$$

METHODS OF NUMERICAL INTEGRATION

Two methods are developed to solve the differential equations (25). In the first method, the differential equations are numerically integrated along r/k, which is considered the independent variable. (In the second method, α is considered the independent variable.) Because many terms in the equations are trigonometric functions of α, the use of α as the independent variable considerably reduces the work of computation.

Numerical integration with r/k as independent variable.—Equation (25) can be written in the following forms:

$$\left.\begin{aligned} \frac{r}{k}\frac{d\alpha}{d\left(\frac{r}{k}\right)}&=\frac{CE-FB}{AE-DB}\\ \frac{r}{k}\frac{d\gamma}{d\left(\frac{r}{k}\right)}&=\frac{FA-CD}{EA-BD} \end{aligned}\right\} \quad (29)$$

At any point, if α and γ are known, $\frac{d\alpha}{d(r/k)}$ and $\frac{d\gamma}{d(r/k)}$ can be calculated by equations (29). At the boundaries or the center, α is known, but γ is determined by the load. Only one value (unknown) of γ corresponding to a particular load exists on each boundary; therefore it is difficult to start the numerical integrations on the boundary with the correct value of γ corresponding to a given load. Also, in plastic problems covering the strain-hardening range, the method of superposition is invalid. Usually, a method of iteration is used to solve the problem (for example, references 3 and 4). In the method presented herein, an arbitrary but unknown constant k has been introduced in equations (18), (21), and (22). For the cases considered, the terms in the equations that involve load are always multiplied by r, so that $\left(\frac{pr}{h_{init}}\right)^2$ can be written as $\left(\frac{pk}{h_{init}}\right)^2\left(\frac{r}{k}\right)^2$ in equations (18) and (26) and $(\omega r)^2$ as $(\omega k)^2\left(\frac{r}{k}\right)^2$ in equations (21) and (27).

The numerical integration then can be started at the inner boundary (or at the center if there is no circular hole at the center) by using the known values of α_o, a desired value of γ_o, and an arbitrary value of $\left(\frac{pk}{h_{init}}\right)^2$ for the membrane or of $(\omega k)^2$ for the rotating disk. The numerical integrations can then be carried out, obtaining values of α and γ at different values of r/k, until α progressively reaches the value that satisfies the outer boundary condition. Because the value of r is known at the boundaries, the value of k can be determined for the selected value of γ_o. The number of points and the formulas used in the calculation depend on the accuracy required (references 19 and 20). If the formula for evaluating definite integrals is applied after using the forward integration formula (references 19 and 20), great accuracy can easily be obtained.

The procedure used herein to obtain solutions is the same for each problem. Calculations are started from the inner boundary (or from the center if there is no circular hole at the center) with the known value of α_o, the desired value of γ_o, and the arbitrary loading term. The parameter α_o is equal to $\pi/2$ at $r/b=0$ for the membrane and for the solid rotating disk and is equal to $\pi/6$ at $r/a=1$ for the infinite plate with a circular hole and for the rotating disk with a hole. The arbitrary loading terms are $\left(\frac{pk}{h_{init}}\right)^2$ and $(\omega k)^2$ for the membrane and the rotating disk, respectively. Then $\left[\frac{d\alpha}{d(r/k)}\right]_o$ and $\left[\frac{d\gamma}{d(r/k)}\right]_o$, corresponding to α_o and γ_o at the inner boundary or the center, are obtained from equations (29). The following formulas for forward integration are used to determine the first approximate values of α and γ at the next point ($\alpha_1{}^*$ and $\gamma_1{}^*$):

$$\left.\begin{aligned}\alpha_1{}^*&=\alpha_o+\left[\left(\frac{r}{k}\right)_1-\left(\frac{r}{k}\right)_o\right]\left[\frac{d\alpha}{d\left(\frac{r}{k}\right)}\right]_o\\ \gamma_1{}^*&=\gamma_o+\left[\left(\frac{r}{k}\right)_1-\left(\frac{r}{k}\right)_o\right]\left[\frac{d\gamma}{d\left(\frac{r}{k}\right)}\right]_o\end{aligned}\right\} \tag{30a}$$

By substitution of $\alpha_1{}^*$ and $\gamma_1{}^*$ into equation (29), approximate values of $\left[\frac{d\alpha}{d\left(\frac{r}{k}\right)}\right]_1$ and $\left[\frac{d\gamma}{d\left(\frac{r}{k}\right)}\right]_1$ are obtained and the second approximate values of α_1 and γ_1 ($\alpha_1{}^{**}$ and $\gamma_1{}^{**}$) can be computed from the following formulas:

$$\left.\begin{aligned}\alpha_1{}^{**}&=\alpha_o+\frac{1}{2}\left[\left(\frac{r}{k}\right)_1-\left(\frac{r}{k}\right)_o\right]\left\{\left[\frac{d\alpha}{d\left(\frac{r}{k}\right)}\right]_o+\left[\frac{d\alpha}{d\left(\frac{r}{k}\right)}\right]_1^*\right\}\\ \gamma_1{}^{**}&=\gamma_o+\frac{1}{2}\left[\left(\frac{r}{k}\right)_1-\left(\frac{r}{k}\right)_o\right]\left\{\left[\frac{d\gamma}{d\left(\frac{r}{k}\right)}\right]_o+\left[\frac{d\gamma}{d\left(\frac{r}{k}\right)}\right]_1^*\right\}\end{aligned}\right\} \tag{30b}$$

The values of $\alpha_1{}^{**}$ and $\gamma_1{}^{**}$ are substituted into equation (29) again in order to calculate the values of $\left[\frac{d\alpha}{d\left(\frac{r}{k}\right)}\right]_1$ and $\left[\frac{d\gamma}{d\left(\frac{r}{k}\right)}\right]_1$. By use of the following formulas for evaluating definite integrals, the volumes of α_1 and γ_1 are calculated:

$$\left.\begin{aligned}\alpha_1&=\alpha_o+\frac{1}{2}\left[\left(\frac{r}{k}\right)_1-\left(\frac{r}{k}\right)_o\right]\left\{\left[\frac{d\alpha}{d\left(\frac{r}{k}\right)}\right]_o+\left[\frac{d\alpha}{d\left(\frac{r}{k}\right)}\right]_1\right\}\\ \gamma_1&=\gamma_o+\frac{1}{2}\left[\left(\frac{r}{k}\right)_1-\left(\frac{r}{k}\right)_o\right.\quad\left.\frac{d\gamma}{d\left(\frac{r}{k}\right)}\right]_o+\left[\frac{d\gamma}{d\left(\frac{r}{k}\right)}\right]_1\Bigg\}\end{aligned}\right\} \tag{30c}$$

This procedure is applied to the next point, and so forth, until the value of α reaches the required value of α_b at the outside boundary ($\alpha_b=2/3\,\pi$ at $r/b=1$ for the membrane, $\alpha_b=\pi/6$ at $r/b=1$ for the rotating disk, and $\alpha_b=\pi/2$ at $r/a=c/a$ for the thin plate with a circular hole). Inasmuch as

$$\left(\frac{r}{k}\right)_{\alpha=\alpha_b}=\frac{b}{k}$$

the loading terms are determined as follows:

For the membrane,

$$\left(\frac{pb}{h_{init}}\right)^2=\left(\frac{pk}{h_{init}}\right)^2\left(\frac{b}{k}\right)^2 \tag{31a}$$

For the rotating disk,

$$(\omega b)^2=(\omega k)^2\left(\frac{b}{k}\right)^2 \tag{31b}$$

For the infinite plate with a circular hole,

$$t_c=\sigma h_c\left(\frac{r+u}{r}\right)_c=\sigma h_{init}e^{-\epsilon_r}=\sigma h_{init}e^{-\frac{\gamma_c}{2\sqrt{2}}} \tag{31c}$$

or for the flat ring radially stressed at the outside diameter b,

$$t_b=(\sigma_r)_b h_b\left(\frac{r+u}{r}\right)_b=(\sigma_r)_b h_{init}e^{-\frac{\gamma_b}{2\sqrt{2}}(\sin\alpha_b-\sqrt{3}\cos\alpha_b)} \tag{31d}$$

where t_c and t_b are the tensions per unit original circumferential length at $r=c$ and $r=b$, respectively.

Numerical integration with α as independent variable.—Equations (29) can be written in the following forms:

$$\left.\begin{aligned}\frac{d\gamma}{d\alpha}&=\frac{FA-CD}{CE-FB}\\ \frac{d\left(\frac{r}{k}\right)}{d\alpha}&=\frac{AE-DB}{CE-BF}\frac{r}{k}\end{aligned}\right\} \tag{32}$$

By use of equations (26) to (28) and expansion of $e^{f(\alpha,\gamma)}$ into a series, the following equations are obtained:

For the circular membrane, from equations (26),

$$\left.\begin{aligned} CE-BF&=2GJ-\left[2\sqrt{3}HJg\left(\alpha,\gamma,\frac{\gamma}{\tau}\frac{d\tau}{d\gamma}\right)f_1(\alpha,\gamma)+2\sqrt{3}\right]j\left(\alpha,\gamma,\frac{r}{k},\frac{pk}{h_{init}}\right)\\ AF-CD&=2\sqrt{2}L-2HJ\gamma-2\sqrt{2}Lf_2(\alpha,\gamma)j\left(\alpha,\gamma,\frac{r}{k},\frac{pk}{h_{init}}\right)\\ AE-BD&=-L^2-J^2g\left(\alpha,\gamma,\frac{\gamma}{\tau}\frac{d\tau}{d\gamma}\right)\end{aligned}\right\} \tag{33}$$

For the rotating disk, from equations (27),

$$\left.\begin{aligned} CE-BF&=-2HL-2\sqrt{3}HJg\left(\alpha,\gamma,\frac{\gamma}{\tau}\frac{d\tau}{d\gamma}\right)f_1(\alpha,\gamma)+L\frac{K_2}{\tau}\left(\frac{r}{k}\right)^2f_3(\alpha,\gamma)\\ AF-CD&=\left\{8H^2-2\sqrt{3}HL[1-f_1(\alpha,\gamma)]+J\frac{K_2}{\tau}\left(\frac{r}{k}\right)^2f_3(\alpha,\gamma)\right\}\gamma\\ AE-BD&=-L^2-J^2g\left(\alpha,\gamma,\frac{\gamma}{\tau}\frac{d\tau}{d\gamma}\right)\end{aligned}\right\} \tag{34}$$

For the infinite plate with a circular hole, from equations (28),

$$\left.\begin{aligned} CE-BF&=-2HL-2\sqrt{3}HJg\left(\alpha,\gamma,\frac{\gamma}{\tau}\frac{d\tau}{d\gamma}\right)f_1(\alpha,\gamma)\\ AF-CD&=\{8H^2-2\sqrt{3}HL[1-f_1(\alpha,\gamma)]\}\gamma\\ AE-BD&=-L^2-J^2g\left(\alpha,\gamma,\frac{\gamma}{\tau}\frac{d\tau}{d\gamma}\right)\end{aligned}\right\} \tag{35}$$

where

$G=\sin\alpha$

$H=\cos\alpha$

$J=\sqrt{3}\sin\alpha-\cos\alpha$

$L=\sqrt{3}\cos\alpha+\sin\alpha$

$K_1=\left(\frac{pk}{h_{init}}\right)^2$

$K_2=\sqrt{\frac{2}{3}}\rho(\omega k)^2$

and

$$f_1(\alpha,\gamma)=\frac{1}{\sqrt{\frac{3}{2}}(\cos\alpha)\gamma}\left[1-e^{-\sqrt{\frac{3}{2}}(\cos\alpha)\gamma}\right]$$

$$=1-\frac{1}{2}\sqrt{\frac{3}{2}}(\cos\alpha)\gamma+\frac{1}{4}(\cos^2\alpha)\gamma^2-\ \ldots$$

$$f_2(\alpha,\gamma)=e^{-\sqrt{\frac{3}{2}}(\cos\alpha)\gamma}$$

$$=1-\sqrt{\frac{3}{2}}(\cos\alpha)\gamma+\frac{1}{2}\times\frac{3}{2}(\cos^2\alpha)\gamma^2-$$

$$\frac{1}{4}\sqrt{\frac{3}{2}}(\cos^3\alpha)\gamma^3+\ \ldots$$

$$=1-\sqrt{\frac{3}{2}}(\cos\alpha)\gamma f_1(\alpha,\gamma)$$

$$f_3(\alpha,\gamma)=e^{\frac{\gamma}{\sqrt{2}}\sin\alpha}$$

$$=1+\left(\frac{1}{\sqrt{2}}\sin\alpha\right)\gamma+\frac{1}{2}\left(\frac{1}{\sqrt{2}}\sin\alpha\right)^2\gamma^2+$$

$$\frac{1}{6}\left(\frac{1}{\sqrt{2}}\sin\alpha\right)^3\gamma^3+\ \ldots$$

$$g\left(\alpha,\gamma,\frac{\gamma}{\tau}\frac{d\tau}{d\gamma}\right)=\frac{\gamma}{\tau}\frac{d\tau}{d\gamma}-\sqrt{\frac{3}{2}}\frac{\gamma}{\sqrt{3}\sin\alpha-\cos\alpha}=\frac{\gamma}{\tau}\frac{d\tau}{d\gamma}-\sqrt{\frac{3}{2}}\frac{\gamma}{J}$$

$$j\left(\alpha,\gamma,\frac{r}{k},\frac{pk}{h_{init}}\right)=\left[1-\frac{e^{\sqrt{\frac{3}{2}}\gamma(\sqrt{3}\sin\alpha+\cos\alpha)}}{6\tau^2(\sqrt{3}\sin\alpha-\cos\alpha)^2}\left(\frac{r}{k}\right)^2\left(\frac{pk}{h_{init}}\right)^2\right]^{1/2}$$

$$=\left[1-\frac{K_1}{6J^2}\left(\frac{1}{\tau}\frac{r}{k}\right)^2\frac{f_3(\alpha,\gamma)}{f_2(\alpha,\gamma)}\right]^{1/2}$$

The symbols G, H, J, and L are trigonometric functions of α only; K_1 and K_2 are arbitrary loading constants. The symbols f_1, f_2, f_3, and g are functions of α and γ; j is a function of α, γ, and r/k.

For the solution of an infinite plate with a circular hole α is the independent variable. The procedure of numerical integration is similar to that used in the method in which r/k is the independent variable. The first four terms of the series of $e^{f(\alpha,\gamma)}$ are used; the accuracy of the result is the same as that of the previous method, but computation is reduced by one half.

Both methods presented herein are used to obtain the solutions for the given values of γ_o. The purpose of the present paper is to obtain solutions for the entire strain-hardening range and the methods developed are very convenient for this purpose. If, however, a solution for only a particular value of loading is required, it can be obtained by interpolating between values obtained from two or three solutions corresponding to loading near the specified value.

NUMERICAL EXAMPLES

Membrane.—In order to compare the results for the circular membrane obtained by the method developed herein with those obtained by Gleyzal (reference 3), one numerical solution for infinitesimal strain is calculated by using the $\tau(\gamma)$ curve of the tensile test in figure 1 of reference 3. Inasmuch as reference 3 states that: "For simplicity, strain will be taken to mean conventional strain $(ds-ds_o)/ds_o$ where ds and ds_o are final and initial arc length, respectively.", equations (25a) and (36) given in appendix A for infinitesimal strain are used. The calculation is started at $r/k=0.005$. Values of $\alpha_o=1.5708$, $\gamma_o=0.0299$, and $pk/h_{\text{init}}=55{,}920$ are used.

Rotating disk.—Numerical solutions for the rotating disk for finite strain (equations (25) and (27)) are calculated. The $\tau(\gamma)$ curves of two materials, Inconel X and 16–25–6, are plotted in figure 5 (a). These data were supplied by W. F. Brown, Jr., H. Schwartzbart, and M. H. Jones. The same $\tau(\gamma)$ curves are plotted on logarithmic coordinates in figure 5 (b). These materials, Inconel X and 16–25–6, for which τ is not a power function of γ, were chosen so that more general information can be obtained. The given octahedral shear stress-strain curves (fig. 5) of these two materials have not been corrected for the triaxiality and nonuniform stress distribution introduced by necking and consequently do not represent the exact stress-strain relation after necking of these two materials. The solutions obtained from the $\tau(\gamma)$ curves of the tensile test after necking can, however, represent the solutions corresponding to materials having the exact $\tau(\gamma)$ curves shown in figure 5 and for simplicity such materials are herein referred to as "Inconel X" and "16–25–6".

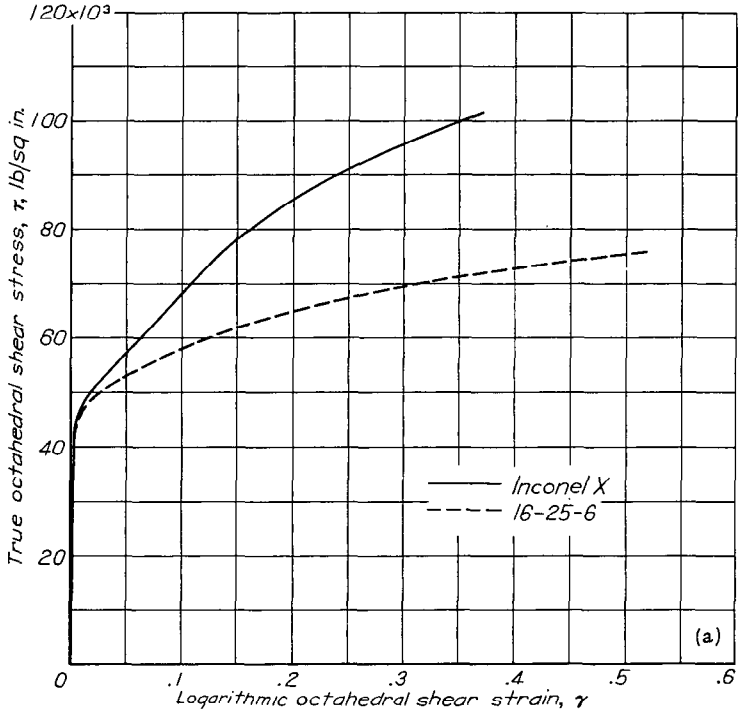

(a) Linear-scale plot.

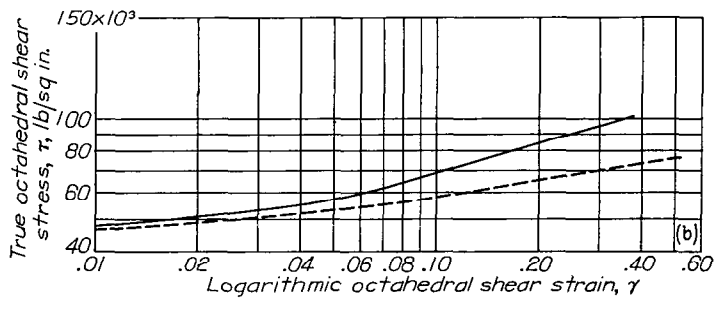

(b) Logarithmic-scale plot.

FIGURE 5.—Octahedral shear stress-strain curves.

The calculation for the solid rotating disk is started at $r/k=0.005$, as in the case of the membrane.

Three solutions are also obtained for the rotating disk with a central hole, using Inconel X. Calculations are started at $r/a=1$.

All numerical examples for the rotating disk are given in the following table:

Solid rotating disk		
Material	γ_o	$K_2=\sqrt{\frac{2}{3}}\rho(\omega k)^2$
Inconel X	0.04 .1152 .30	1×10^5 1×10^5 1×10^5
16–25–6	0.04 .1152 .30	1×10^5 1×10^5 2.5×10^5

Rotating disk with central hole		
Material	γ_o	$\sqrt{\frac{2}{3}}\rho(\omega a)^2$
Inconel X	0.30 .30 .30	1×10^4 2×10^3 4×10^2

Infinite plate with circular hole.—The calculations for the infinite plate with a circular hole are carried out for the case in which $\sigma_r=0$ at $r/a=1$. The value of α_o at $r/a=1$ is then equal to 0.5236. (When σ_r is different from 0 at $r/a=1$, the corresponding value of α_o should be used.) The same materials as in the previous problem are considered. The numerical examples are:

Material	γ_o
Inconel X	0.04 .1152 .1871 .30
16–25–6	0.04 .1871 .30

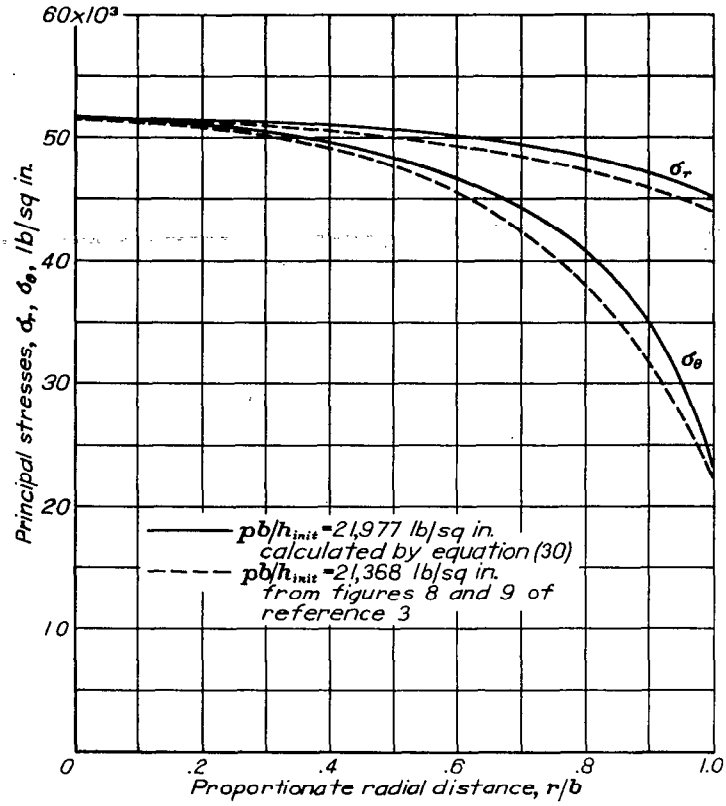

FIGURE 6.—Variation of principal stresses with proportionate radius distance.

RESULTS AND DISCUSSIONS

The radial and circumferential stresses σ_r and σ_θ, respectively, obtained for the circular membrane are plotted against r/b in figure 6. Two curves, taken from reference 3, corresponding to calculations for about the same pressure used in the present calculation, are included in the figure for comparison. In the present calculation, the $\tau(\gamma)$ curve given in figure 1 of reference 3 and the same infinitesimal-strain definition based on the original dimension are used. The initial thickness h_{init} is also used for consistency in the calculation rather than the instantaneous thickness h, which is used in reference 3.

The variations of α with the radius for the rotating disk and with the radius for the infinite plate with a circular hole are plotted in figures 7 (a) and 7 (b), respectively, for different loads and materials. The variations of α with γ_o (or loading) at various radii for the rotating disk and the infinite plate with a circular hole are plotted in figures 8 (a) and 8 (b), respectively. Similar curves for the ratio of the principal stresses σ_r/σ_θ are shown in figures 9 (a), 9 (b), and 10. Comparison of figure 7 and figures 9 (a) and 9 (b) shows that the variations of α with radius are very similar to the variations of σ_r/σ_θ with radius, although the relation between α and σ_r/σ_θ is not linear.

Numerical examples for a membrane with a large strain are not calculated herein, because the result of reference 3 is sufficient to give an approximate variation of the ratios of principal stresses along the radius during loading, although the infinitesimal-strain concept is used. The variations of the ratio of principal stresses with radius for different loads, based on the values of σ_r and σ_θ given in figures 8 and 9 of reference 3, are calculated and plotted on figure 9 (c).

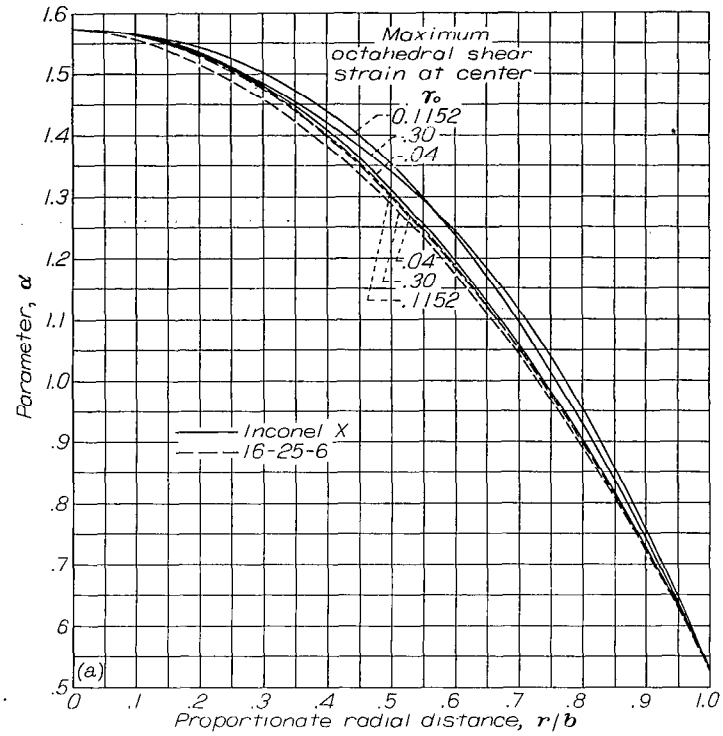

(a) Rotating disk.

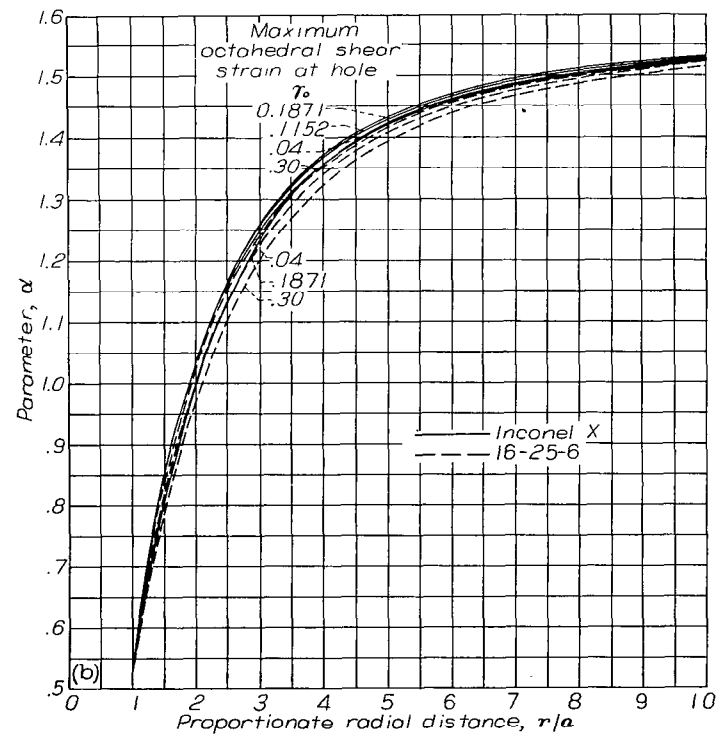

(b) Infinite plate with hole.

FIGURE 7.—Variations of parameter α with proportionate radius distance for Inconel X and 16-25-6.

The values of σ_r are plotted against σ_θ at various radii under different loads for the rotating disk and the infinite plate with a circular hole in figures 11 (a) and 11 (b). The heavy solid and dashed curves represent the values of σ_r and σ_θ at different radii for any given load and are called loading curves. The loading curve moves away from the

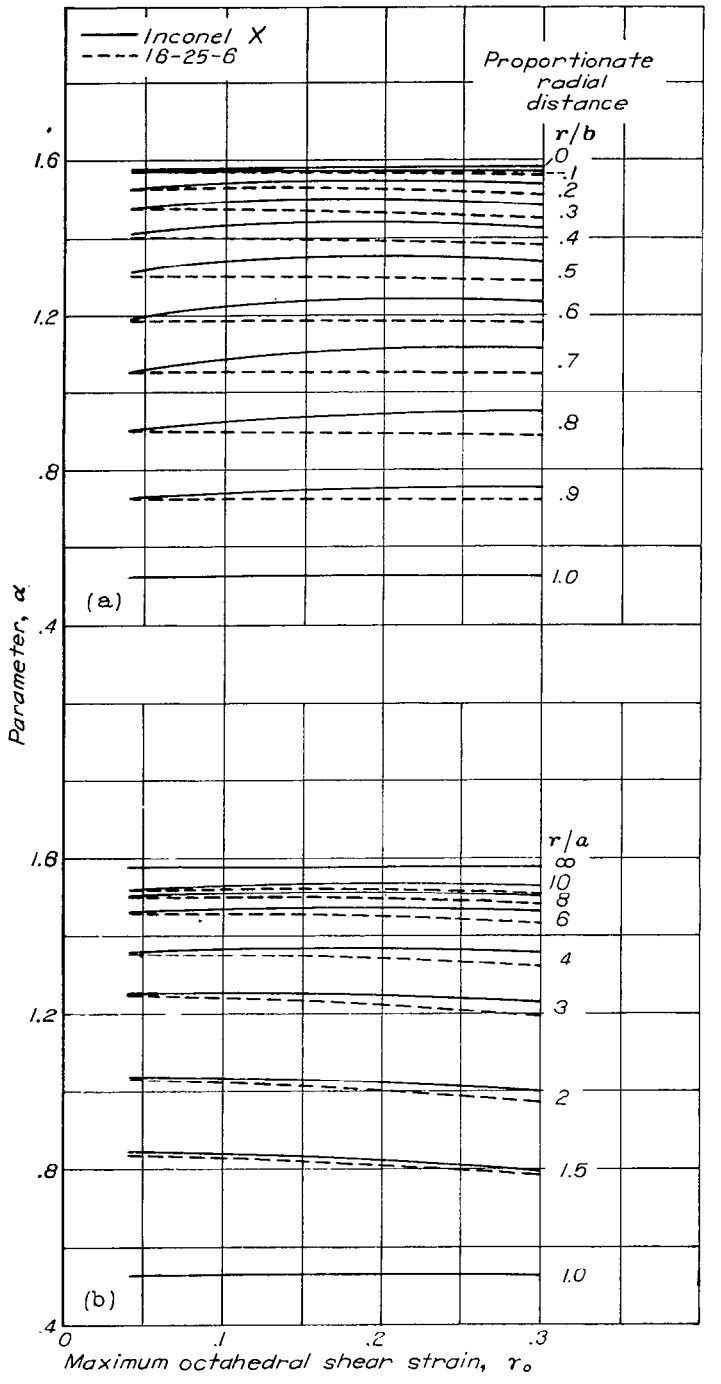

(a) Rotating disk.
(b) Infinite plate with hole.

FIGURE 8.—Variation of parameter α with maximum octahedral shear strain at different radii.

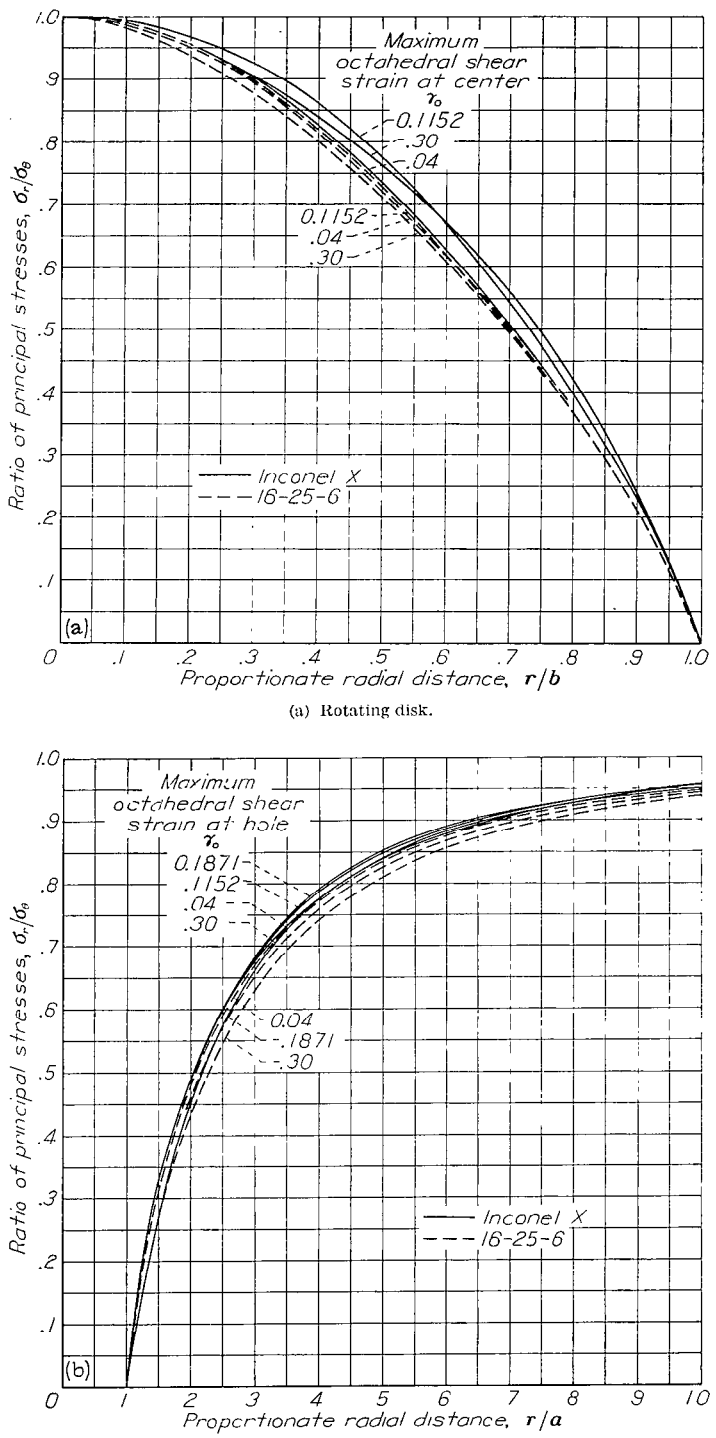

(a) Rotating disk.

(b) Infinite plate with hole.

FIGURE 9.—Variations of ratio of principal stresses with proportionate radial distance.

origin with increasing load. The light solid and dotted lines connecting the different loading curves at a given radius and extending to the origin represent the values of σ_r and σ_θ at different loads for any given radius and are called loading paths. Also shown in the figures are the yielding surfaces, which are ellipses under the deformation theory.

A clear picture of the variation of the ratios of principal stresses in this group of problems with different loads for Inconel X, 16–25–6, and the material used in reference 3 is given in figures 7 to 11. It is evident that the ratios of principal stresses remain essentially constant during loading. The deformation theory is therefore applicable to this group of problems, at least for the materials considered.

The variations of γ and γ/γ_o with radius are plotted in figures 12 and 13, respectively, for the rotating disk and the infinite plate with a circular hole. It is interesting to note that the curves in figure 13 for different loads for the same material are quite close together. For different materials, the curves of figures 7 and 9 are also close, but the curves of figure 13 are not as close together.

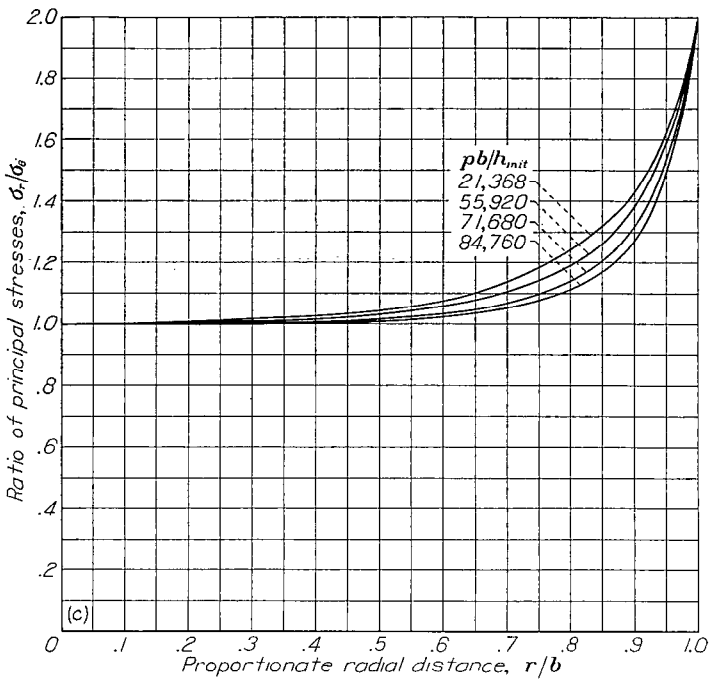

(c) Circular membrane under pressure.

FIGURE 9.—Concluded. Variations of ratio of principal stresses with proportionate radial distance.

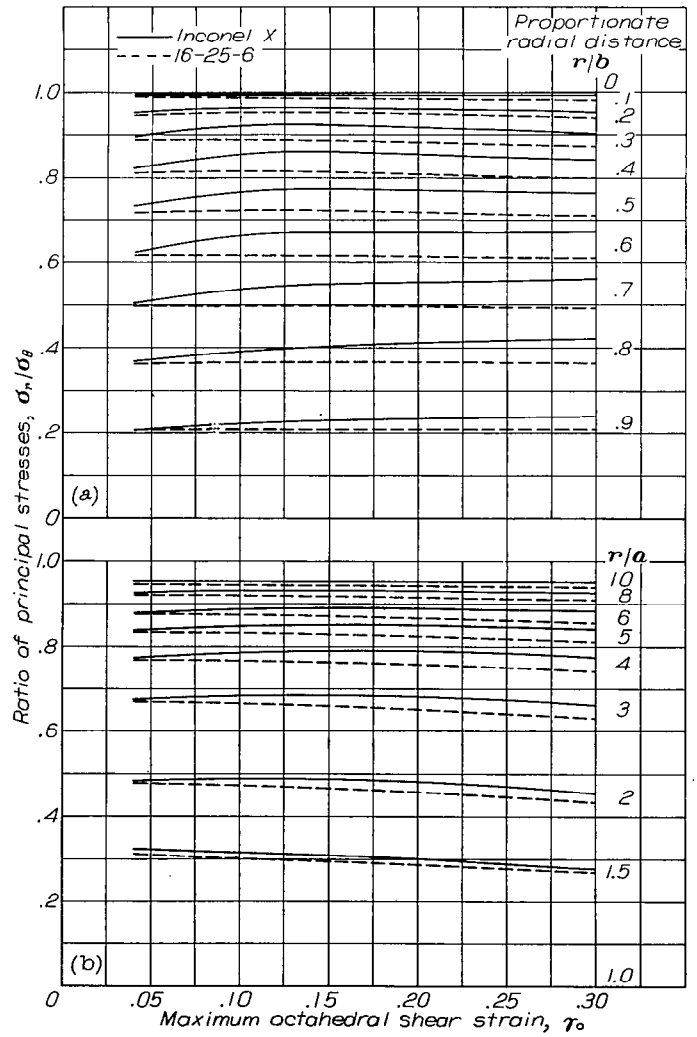

(a) Rotating disk. (b) Infinite plate with hole.

FIGURE 10.—Variation of ratio of principal stresses with maximum octahedral shear strain at different radii.

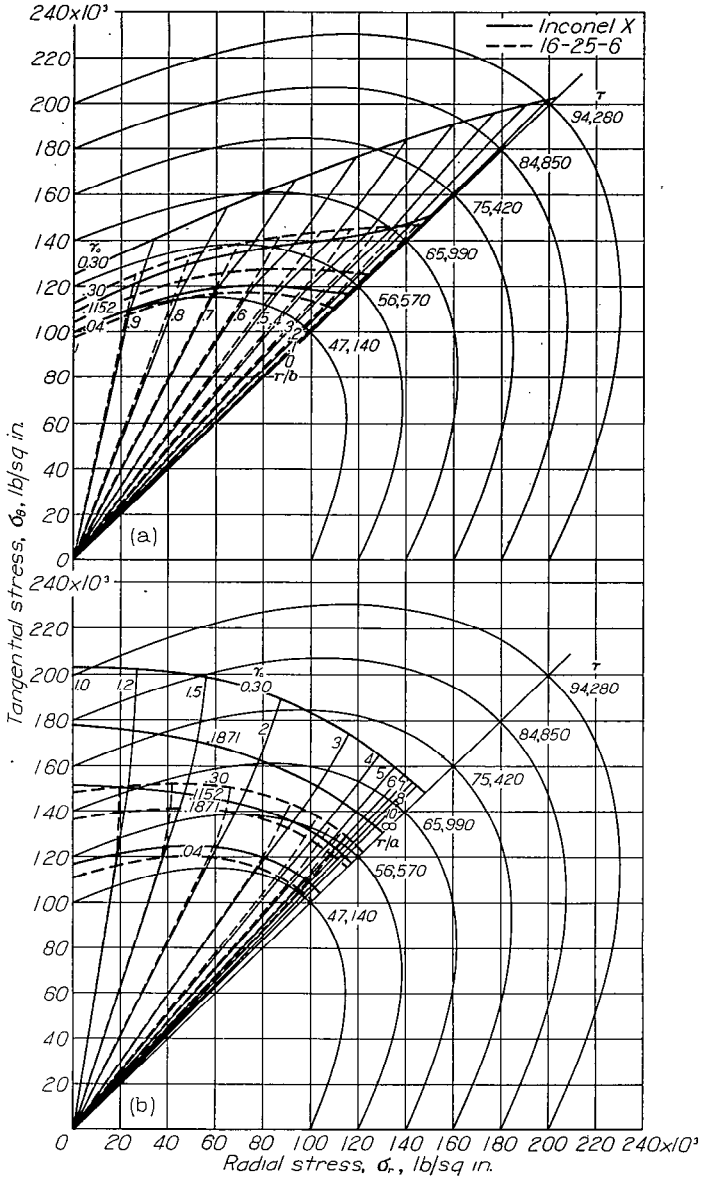

(a) Rotating disk.
(b) Infinite plate with circular hole.

FIGURE 11.—Loading curves, loading paths, and yielding surfaces.

The distributions of principal stresses and principal strains along the radius for the rotating disk and for the infinite plate with a circular hole are plotted in figures 14 and 15, respectively. For comparison, the variations of $\sigma_\theta/(\sigma_\theta)_b$, $\epsilon_\theta/(\epsilon_\theta)_b$, and γ/γ_b with radius for both the elastic and the plastic range are plotted in figures 16 and 17. (The equations for the elastic case are given in appendix B.) If only the stress distributions for the elastic and plastic cases are compared (figs. 16 (a) and 17 (a)), it is seen that the stresses are more uniform in the plastic state; but if the distributions of the principal strains and the octahedral shear strain for the elastic and the plastic cases are compared (figs. 16 (b), 16 (c), 17 (b), and 17 (c)), it is evident that a less-uniform strain distribution is obtained in the plastic state. It is of special interest in the case of the finite plate with a hole to note that with plastic deformation and stress-(tangential stress) concentration factor around the hole is reduced; instead there is a high concentration in principal strain and in octahedral shear

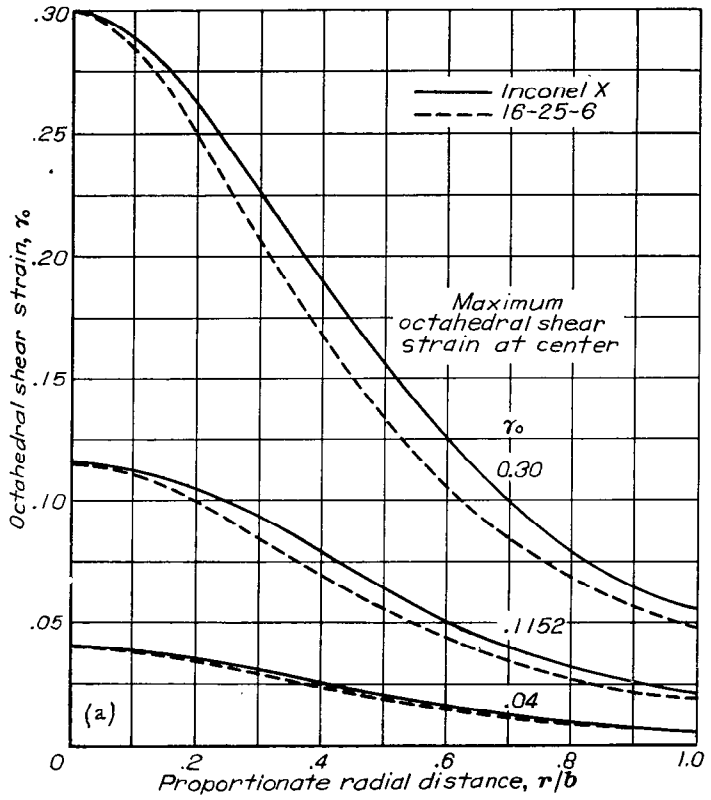

(a) Rotating disk.

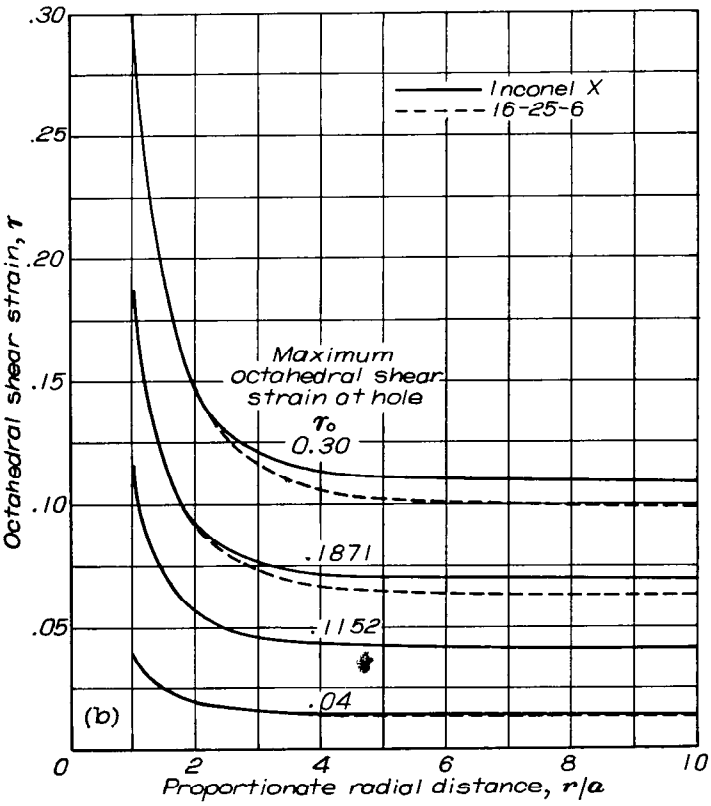

(b) Infinite plate with hole.

FIGURE 12.—Variation of octahedral shear strain with proportionate radial distance.

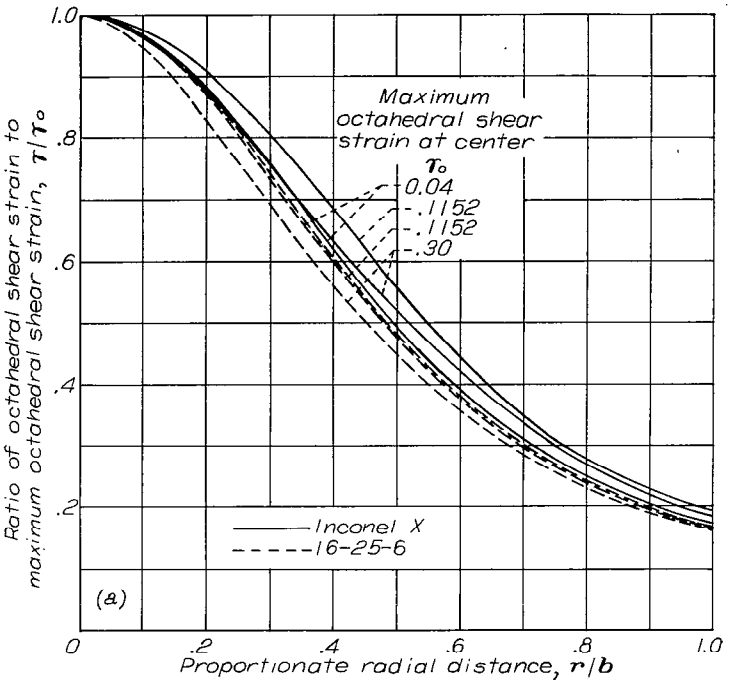

(a) Rotating disk.

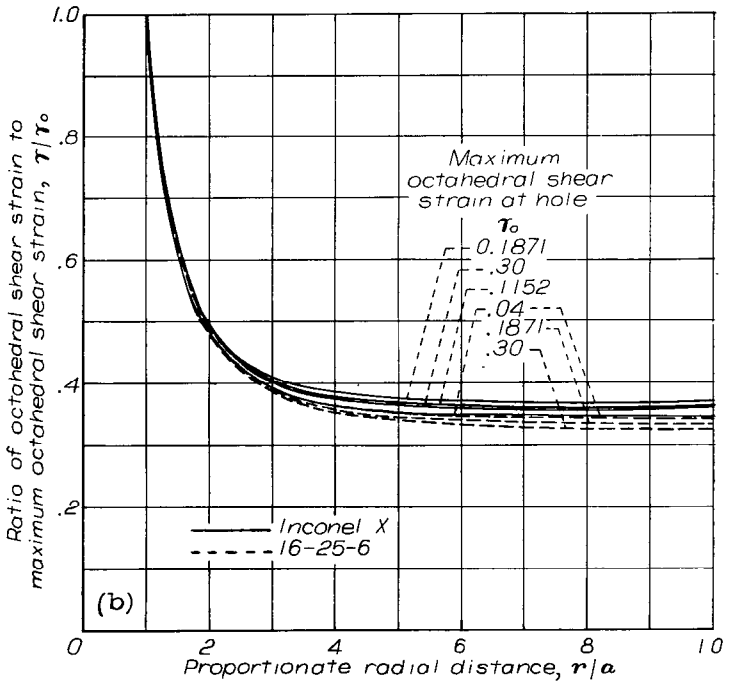

(b) Infinite plate with hole.

FIGURE 13.—Variation of ratio of octahedral shear strain to maximum octahedral shear strain with proportionate radial distance.

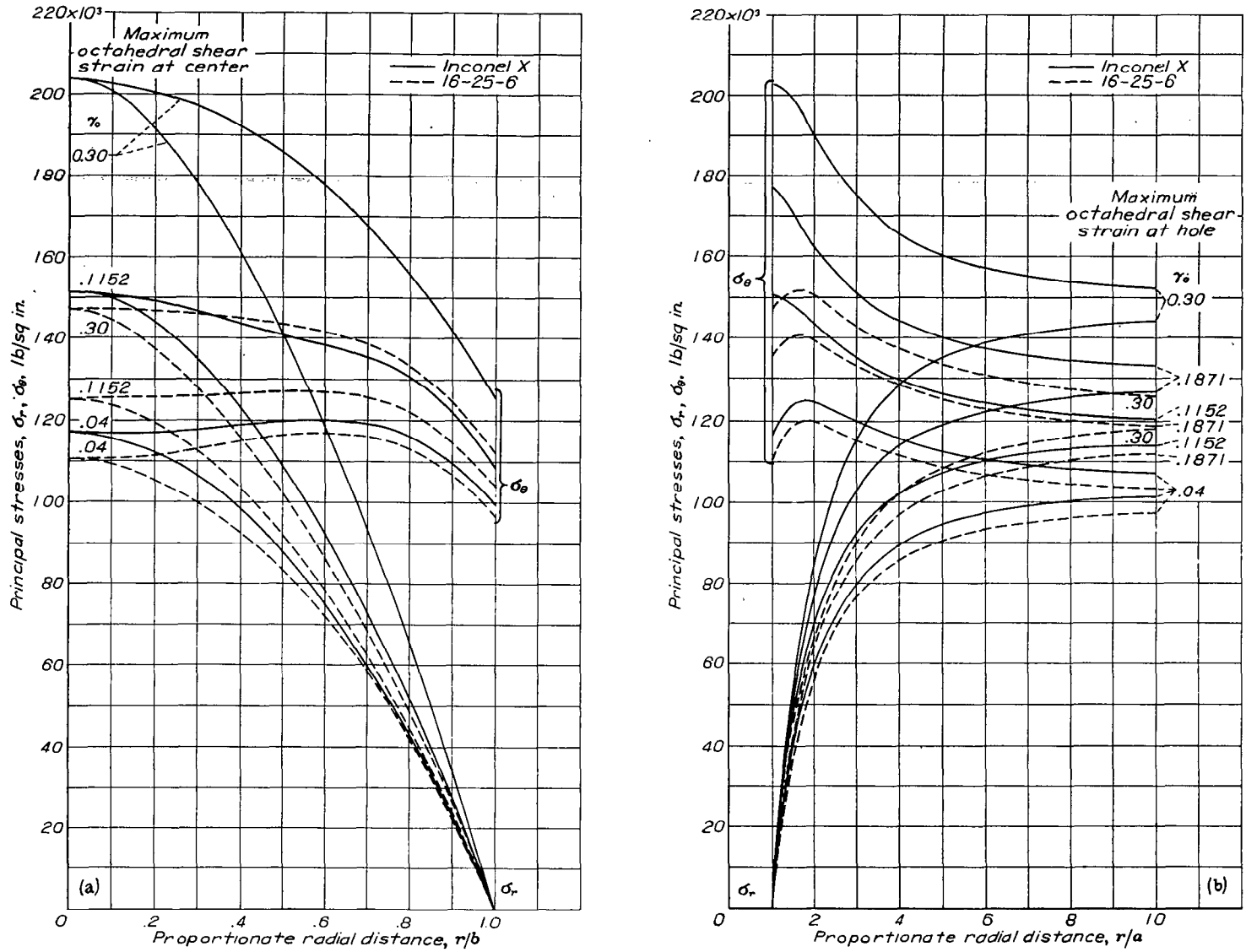

(a) Rotating disk.

(b) Infinite plate with hole.

FIGURE 14.—Variation of principal stresses with proportionate radial distance.

strain. A similar conclusion regarding the concentration factor around a circular hole in a tension panel is given in references 21 and 22.

The quantities $\sigma_\theta/(\sigma_\theta)_o$, $\sigma_r/(\sigma_r)_o$, $\epsilon_r/(\epsilon_r)_o$, and $\epsilon_\theta/(\epsilon_\theta)_o$ along the radius for the rotating disk and $\sigma_\theta/(\sigma_\theta)_o$ and $\epsilon_\theta/(\epsilon_\theta)_o$ for the infinite plate with a circular hole are plotted in figures 18 and 19, respectively. The curves representing $\sigma_r/(\sigma_r)_o$, $\epsilon_r/(\epsilon_r)_o$, and $\epsilon_\theta/(\epsilon_\theta)_o$ for Inconel X and 16–25–6 and different values of γ_o are close together; but the curves of $\sigma_\theta/(\sigma_\theta)_o$ are quite far apart for the two materials, as well as for different values of γ_o.

The relation between the rotating-speed function $\rho(\omega b)^2$ and γ_o for the rotating disk and the relation between the tension per unit original circumferential length t_b/h_{init} and γ_o for the infinite plate with a hole are plotted in figures 20 (a) and 20 (b), respectively. It is shown in these figures that $\rho(\omega b)^2$ and t_b/h_{init} increase considerably for Inconel X and increase only slightly for 16–25–6 as the value of γ_o increases from 0.04 to 0.30.

Figures 7, 13, and 16 to 19 show that for the plate with a hole, the variations of α, γ/γ_o, $\epsilon_r/(\epsilon_r)_o$, and $\epsilon_\theta/(\epsilon_\theta)_o$ with radius are essentially independent of the value of γ_o for the plate and the $\tau(\gamma)$ curve of the material, at least for the materials considered. These results show that the deformation that

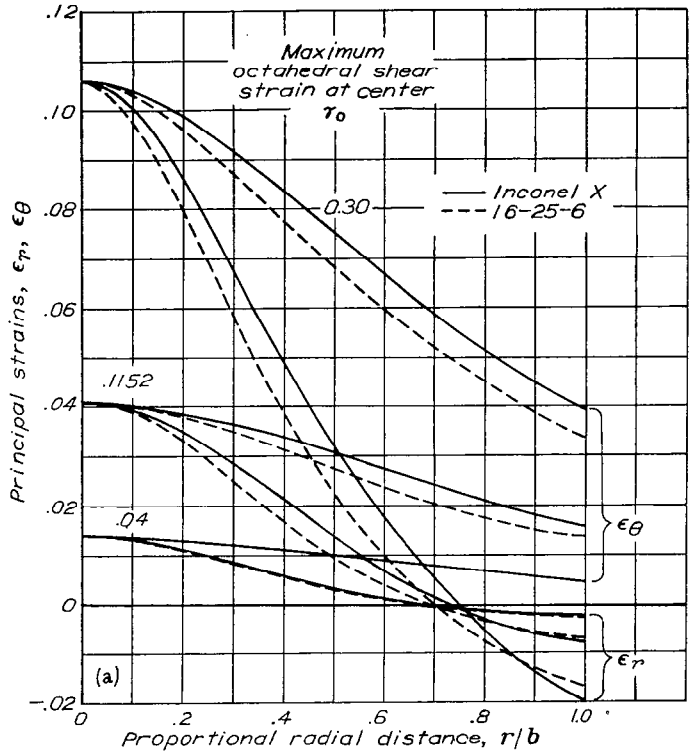

(a) Rotating disk.

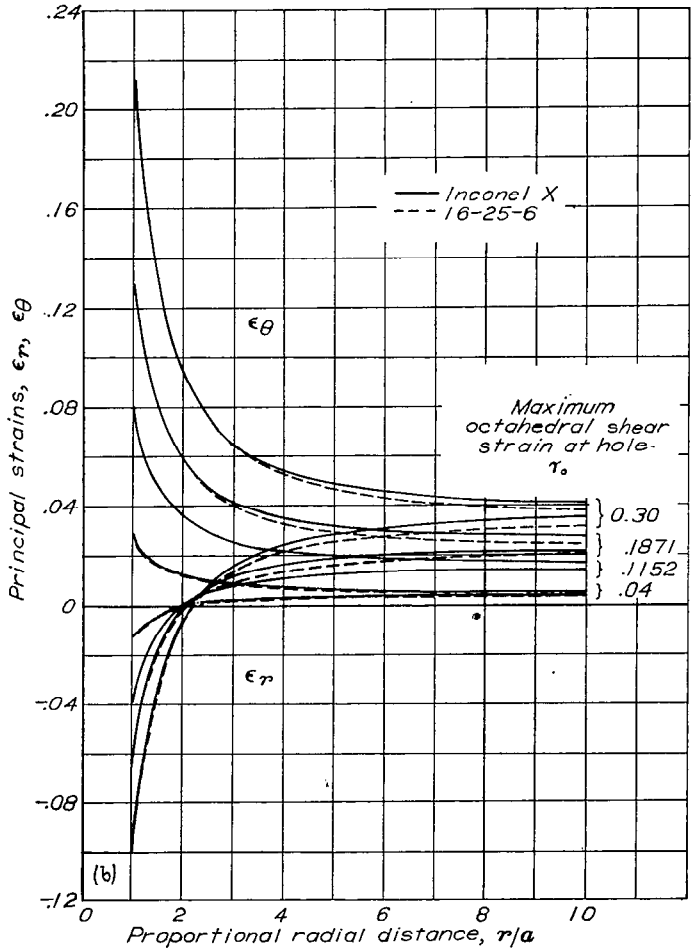

(b) Infinite plate with hole.

FIGURE 15.—Variation of principal strains with proportionate radial distance.

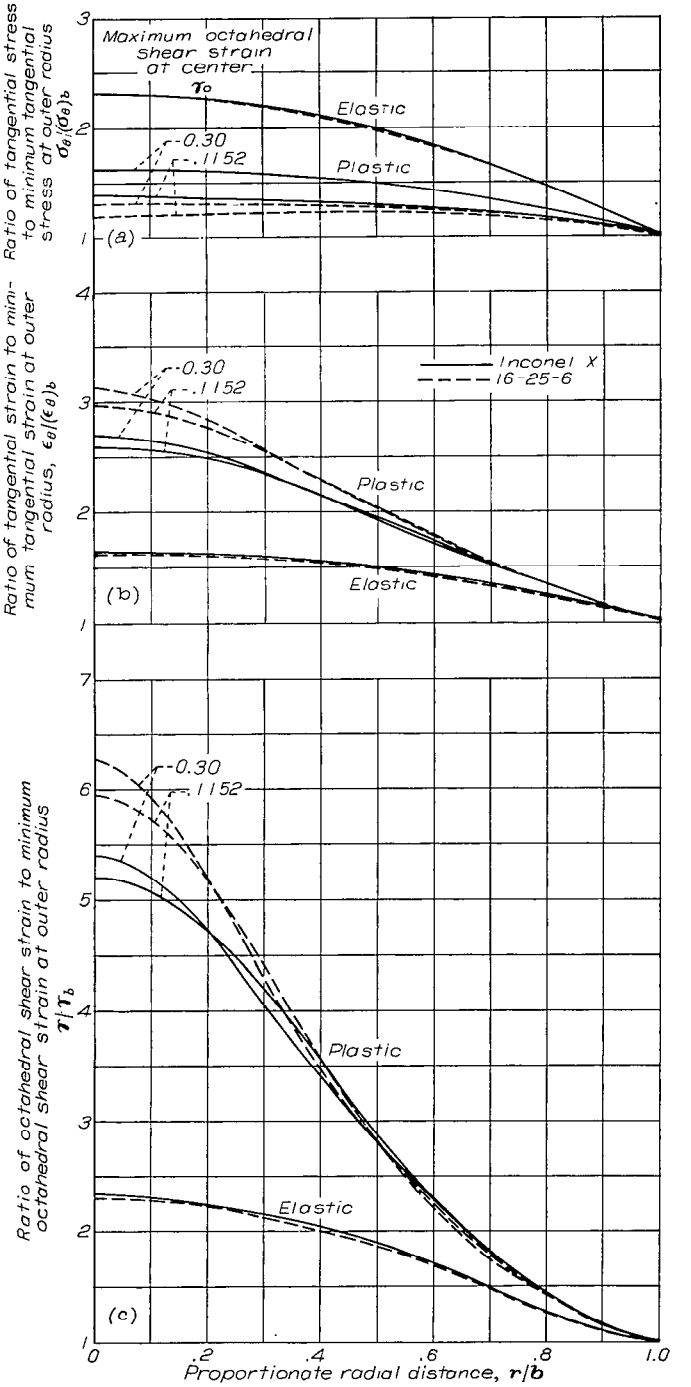

(a) Variation of ratio of tangential stress to minimum tangential stress at outer radius with proportionate radial distance.

(b) Variation of ratio of tangential strain to minimum tangential strain at outer radius with proportionate radial distance.

(c) Variation of ratio of octahedral shear strain to minimum octahedral shear strain at outer radius with proportionate radial distance.

FIGURE 16.—Comparison of results obtained in elastic and plastic range for rotating disk.

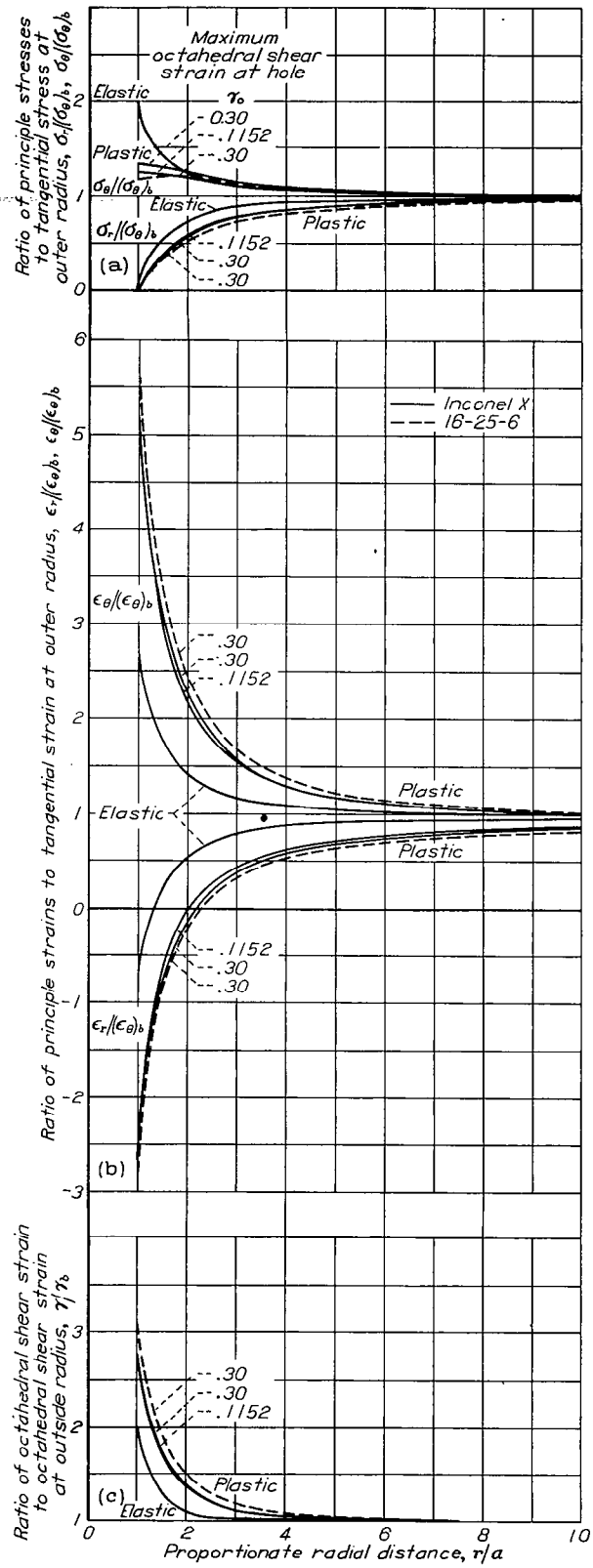

(a) Variation of ratio of principal stresses to tangential stress at outer radius with proportionate radial distance.

(b) Variation of ratio of principal strains to tangential strain at outer radius with proportionate radial distance.

(c) Variation of ratio of octahedral shear strain to octahedral shear strain at outer radius with proportionate radial distance.

FIGURE 17.—Comparison of results obtained in elastic and plastic range for infinite plate with circular hole.

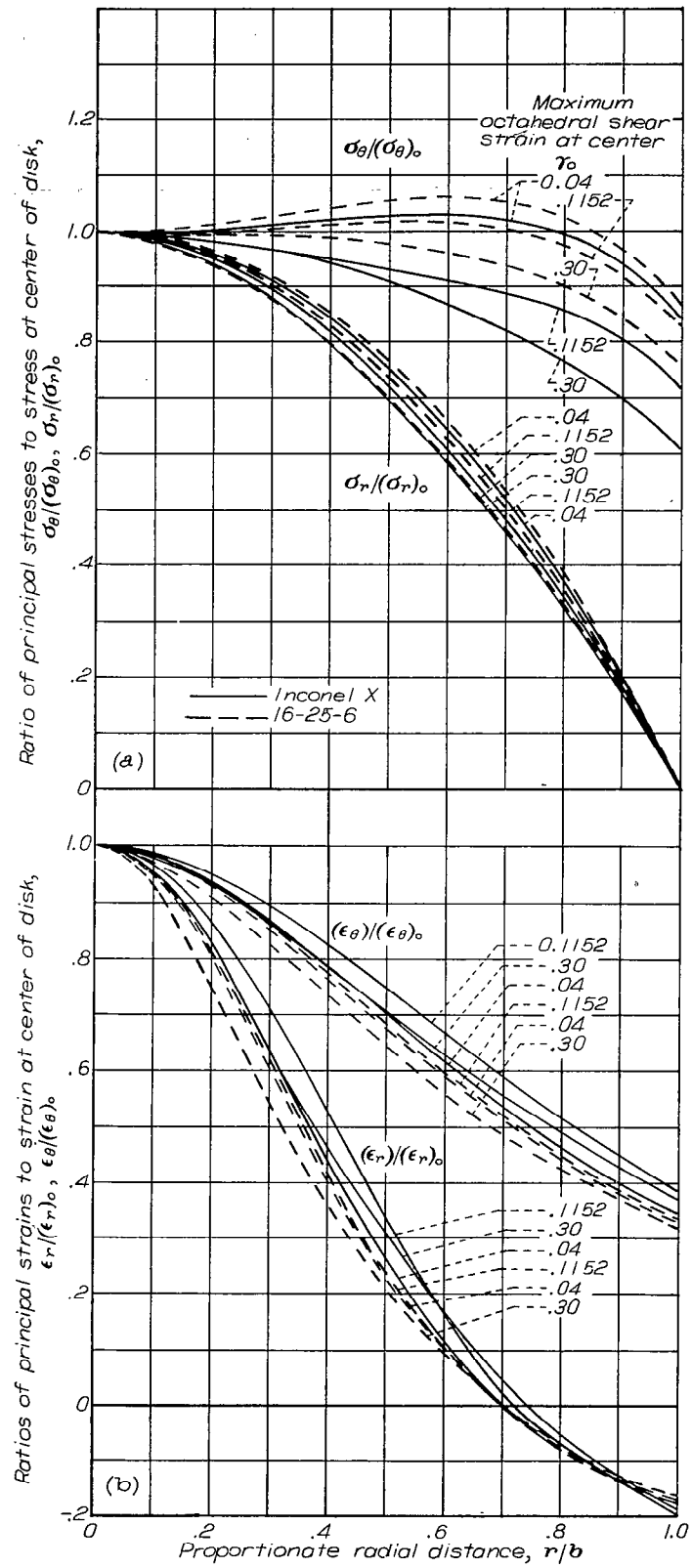

(a) Variation of ratio of principal stresses to stress at center of disk with proportionate radial distance.

(b) Variation of ratios of principal strains to strain at center of disk with proportionate radial distance.

FIGURE 18.—Comparison of stress and strain distributions for different materials and for different maximum octahedral shear strains of rotating disk.

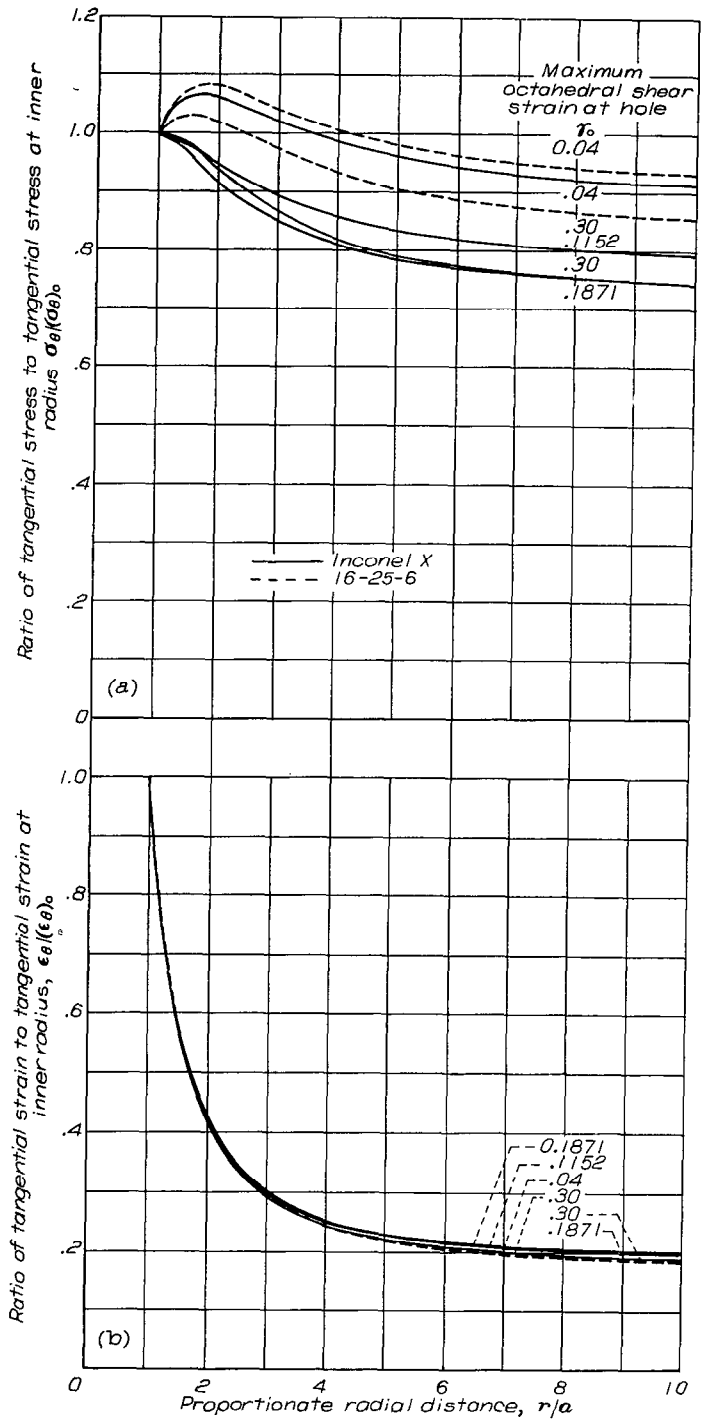

(a) Variation of ratio of tangential stress to tangential stress at inner radius with proportionate radial distance.

(b) Variation of ratio of tangential strain to tangential strain at inner radius with proportionate radial distance.

FIGURE 19.—Comparison of stress and strain distributions for different materials and for different maximum octahedral shear strains of infinite plate with circular hole.

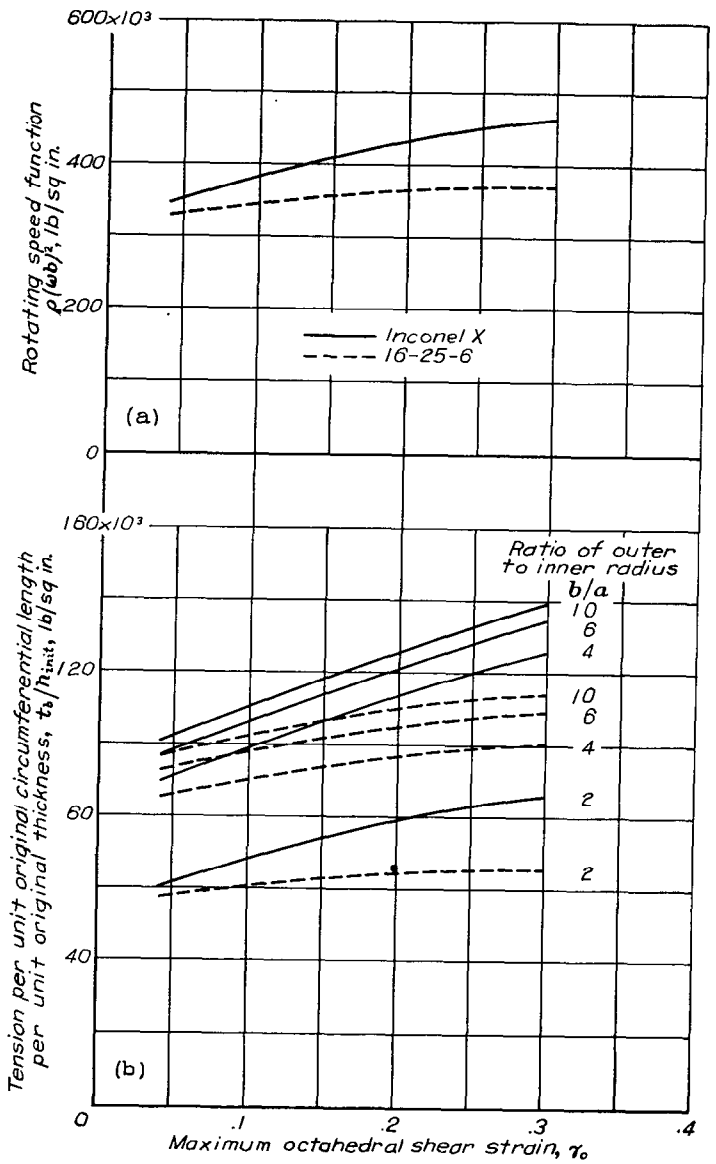

(a) Solid rotating disk.

(b) Flat ring radially stressed.

FIGURE 20.—Relation between rotating-speed function and maximum octahedral shear strain for disk and relation between tension per unit original circumferential length for plate.

can be accepted by the plate before failure depends mainly on the maximum octahedral shear strain (or ductility) of the material, which would not be true if the strain distributions were a function of the $\tau(\gamma)$ curve. For the rotating disk, however, a slight effect of γ_o and the $\tau(\gamma)$ curve is apparent on the strains; this effect seems to be caused by the body-force term of the disk.

The stress distribution that will determine the load which a member can sustain is now considered. Figures 16 to 19 show that the variation of $\sigma_\theta/(\sigma_\theta)_o$ with radius depends on the $\tau(\gamma)$ curve of the material and on the value of γ_o for the member. Figure 20 indicates that the load also depends on the $\tau(\gamma)$ curve. It therefore follows that the added load that the member can sustain between the onset of yielding and failure depends on the $\tau(\gamma)$ curve of the material. The octahedral shear (or effective) stress and strain curve of the material should be used as a criterion in selecting a material

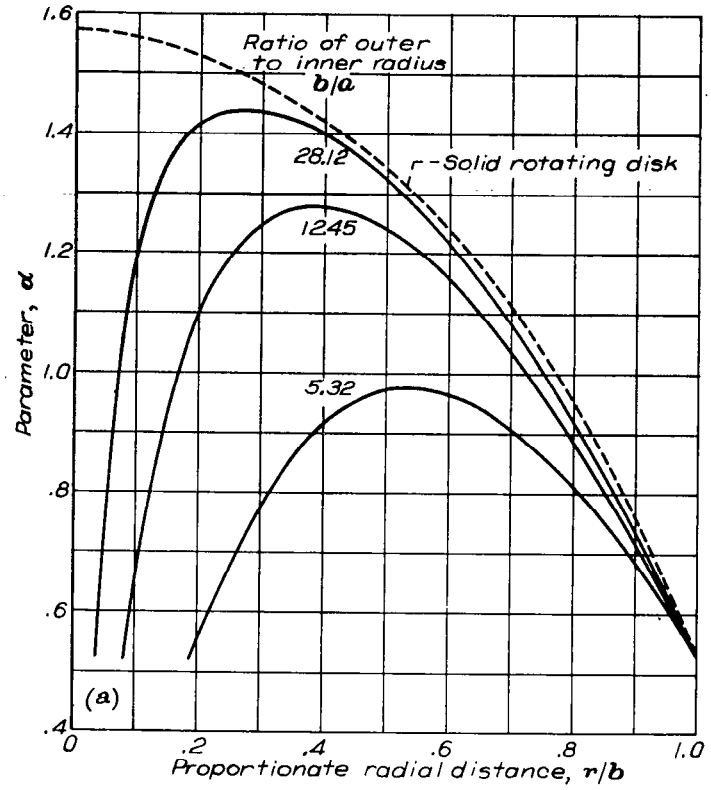

(a) Variation of parameter α with proportionate radial distance.

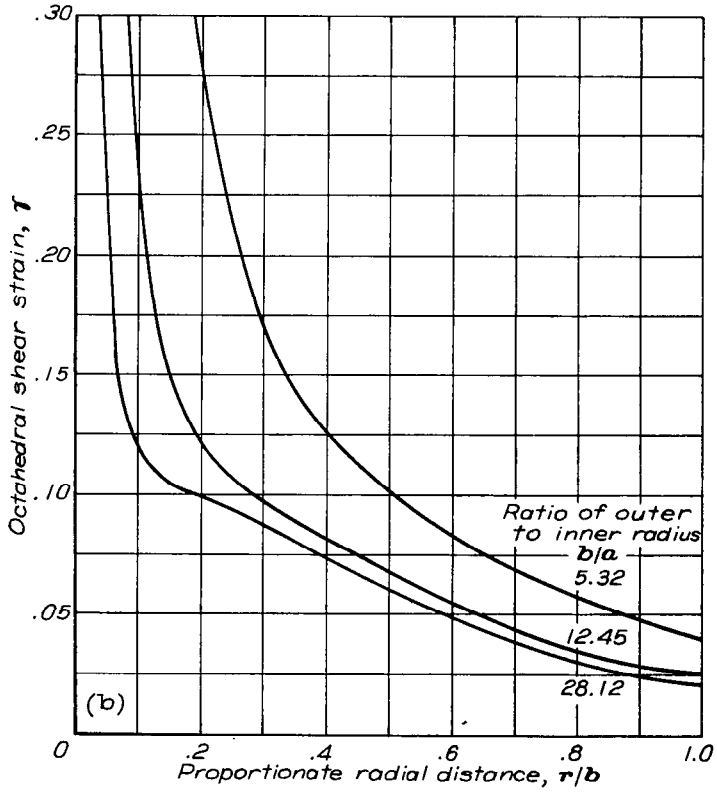

(b) Variation of octahedral shear strain with proportionate radial distance.

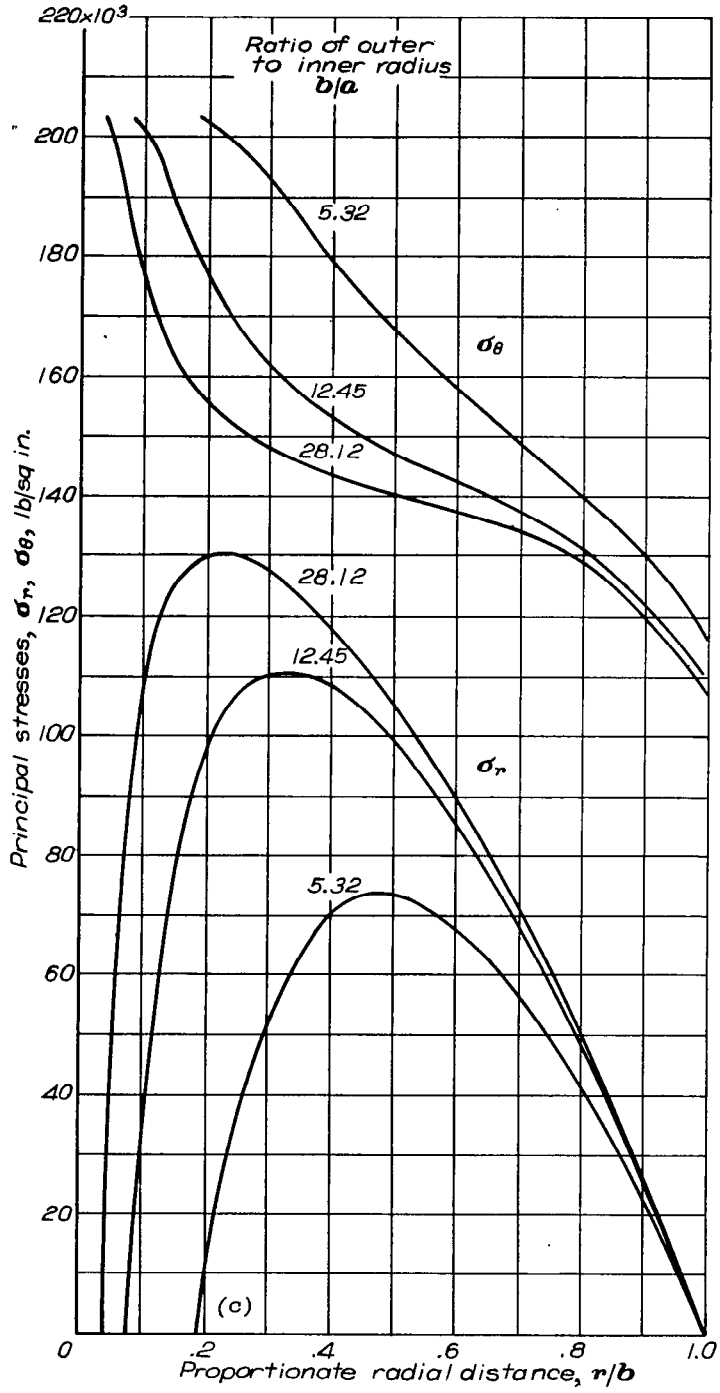

(c) Variation of principal stresses with proportionate radial distance.

FIGURE 21.—Rotating disk with hole. Inconel X; γ_0, 0.3000.

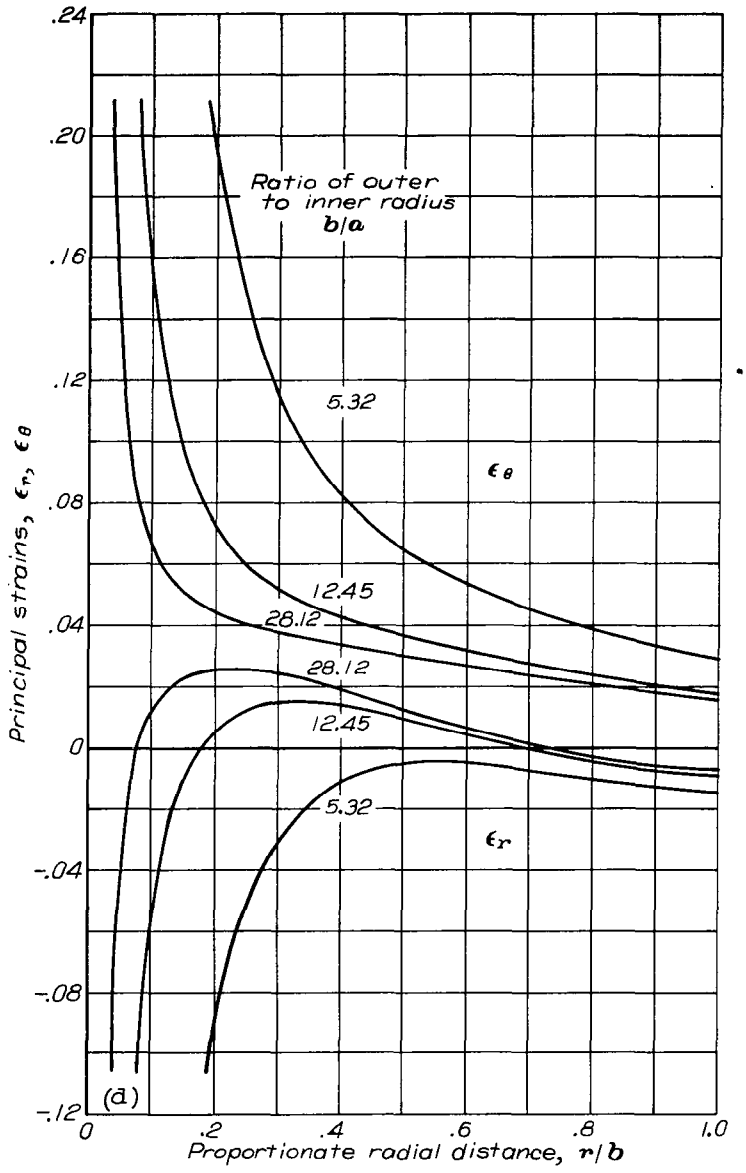

(d) Variation of principal strains with proportionate radial distance.

FIGURE 21.—Continued. Rotating disk with hole. Inconel X; γ_o, 0.3000.

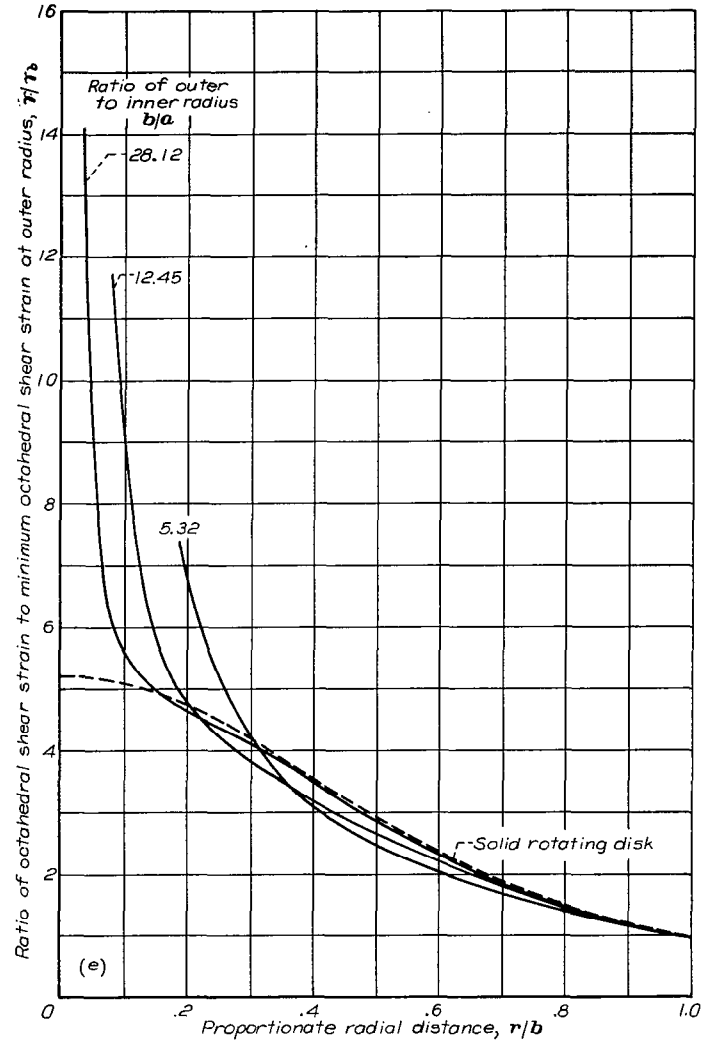

(e) Variation of ratio of octahedral shear strain to minimum octahedral shear strain at outer radius with proportionate radial distance.

FIGURE 21.—Concluded. Rotating disk with hole. Inconel X; γ_o, 0.3000.

for a particular member under a particular loading condition, because consideration of the maximum octahedral shear strain only (or ductility only) of the material is insufficient.

The variations of α, γ, σ_r, σ_θ, ϵ_r, ϵ_θ, and γ/γ_b with radius for three rotating disks with a hole are shown in figure 21. The values of the ratios of outer to inner radius b/a of these three disks equal 5.32, 12.45, and 28.12. These disks were made of Inconel X and had a maximum octahedral shear strain γ_o of 0.3 at the inner radius of the disk. The tangential stress σ_θ, the tangential strain ϵ_θ, and the octahedral shear strain γ are much less uniform for the disk with a hole than for a solid rotating disk. The ratio of maximum to minimum octahedral shear strain γ_o/γ_b is equal to 7.41 for a disk with $b/a=5.32$, 11.75 for a disk with $b/a=12.45$, and 14.1 for a disk with $b/a=28.12$; for a solid disk of the same material, the ratio γ_o/γ_b is about 5.3.

The load, rotating-speed function $\rho(\omega b)^2$, for disks of Inconel X reaching a maximum octahedral shear strain γ_o of 0.3 at the inner radius of the disk and having different ratios of inner to outer radius a/b is represented by the solid curve

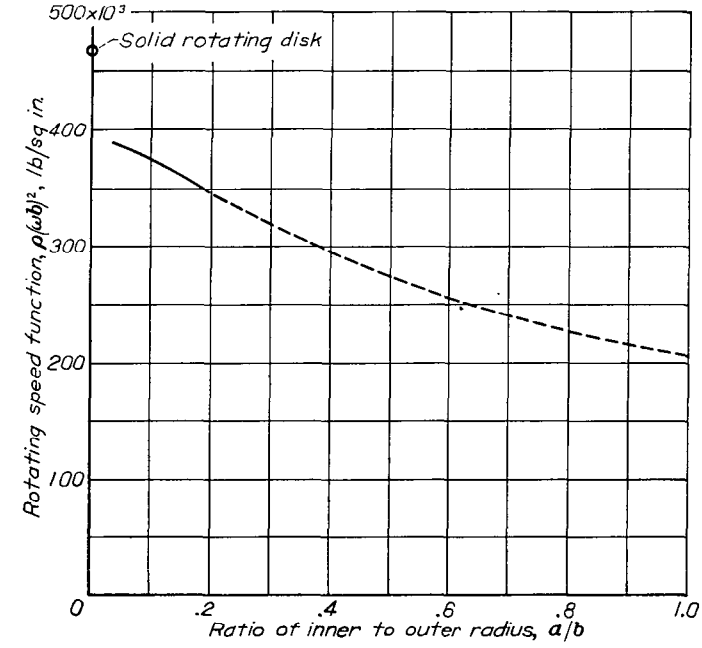

FIGURE 22.—Variation of load (function of speed) with ratio of inner to outer radius of rotating disk with hole. Inconel X; γ_o=0.3000.

in figure 22. The dashed curve in figure 22 is obtained by extending this solid curve toward $a/b=1$, where the value of $\rho(\omega b)^2$ can be determined by considering a rotating ring with $a/b\rightarrow 1$. The figure indicates approximately how the load $\rho(\omega b)^2$ varies with disks having different ratios of inner to outer radius and reaching the same maximum octahedral shear strain at the inner radius of the disk. The value of $\rho(\omega b)^2$ for a solid rotating disk made of Inconel X with $\gamma_o=0.3$ at the center of the disk is indicated in the same figure.

CONCLUSIONS

The results obtained for a membrane, a rotating disk without and with a hole, and an infinite plate with a hole strained in the strain-hardening range in which the elastic strains are negligible compared with the plastic strains for Inconel X and 16–25–6 in the absence of time and temperature effects and unloading show that:

(1) The method developed not only accurately solves the plane-plastic-stress problems with axial symmetry in a simple manner but also shows clearly the octahedral shear strain distribution and the ratio of principal stresses during loading.

(2) The ratio of the principal stresses in the cases investigated remained essentially constant during loading and, consequently, the deformation theory is applicable to this group of problems for the materials considered.

(3) The distributions of principal strains and octahedral shear strains in the plastic state are less uniform than those in the elastic state, although the distributions of tangential stresses appear more uniform in the plastic state. The stress concentration factor around a hole is reduced in the plastic state, but instead there is a high concentration of principal strain and octahedral shear strain.

(4) The ratios of the strains along the radius to their maximum value are essentially independent of the value of the maximum octahedral shear strain of the member and the octahedral shear stress-strain curve of the material. Hence, the deformation that can be sustained by the member before failure depends mainly on the maximum octahedral shear strain (or ductility) of the material.

(5) The stress distributions depend on the octahedral shear stress-strain curve of the material. Hence, the added load that the member can sustain between the onset of yielding and failure depends mainly upon the octahedral shear (or effective) stress-strain curve in the strain-hardening range of the material.

LEWIS FLIGHT PROPULSION LABORATORY
NATIONAL ADVISORY COMMITTEE FOR AERONAUTICS
CLEVELAND, OHIO, *February 28, 1950*

APPENDIX A

EQUATIONS OF EQUILIBRIUM AND COMPATIBILITY FOR INFINITESIMAL STRAIN IN TERMS OF α AND γ

The final forms of the equilibrium and compatibility equations for small strains are given in this section. The concept of infinitesimal strain is defined as follows: The changes of dimensions are small compared with the original dimensions but are large enough so that the elastic strain can be neglected. The equations presented can be obtained either by direct derivation as was done previously or by reducing the equations for finite strains through expanding the $e^{f(\alpha,\gamma)}$ terms in series and neglecting the small terms. For infinitesimal strain, the coefficients (functions of α and γ) A, B, C, D, E, and F of equations (25) are each denoted by a superscript prime but the coefficients (functions of α and γ) are simpler than those for large strain.

$$A'\frac{r}{k}\frac{d\alpha}{d\left(\frac{r}{k}\right)}+B'\frac{r}{k}\frac{d\gamma}{d\left(\frac{r}{k}\right)}=C'$$

$$D'\frac{r}{k}\frac{d\alpha}{d\left(\frac{r}{k}\right)}+E'\frac{r}{k}\frac{d\gamma}{d\left(\frac{r}{k}\right)}=F' \qquad (25a)$$

For the circular membrane under pressure,

$$\left.\begin{aligned} A'&=\sqrt{3}\cos\alpha+\sin\alpha\\ B'&=(\sqrt{3}\sin\alpha-\cos\alpha)\frac{1}{\tau}\frac{d\tau}{d\gamma}\\ C'&=2\cos\alpha\\ D'&=(\sqrt{3}\sin\alpha-\cos\alpha)\gamma\\ E'&=-(\sqrt{3}\cos\alpha+\sin\alpha)\\ F'&=2\sqrt{3}\gamma\cos\alpha+\frac{\sqrt{2}}{6}\left[\frac{\frac{pk}{h_{init}}\frac{r}{k}}{\tau(\sqrt{3}\sin\alpha-\cos\alpha)}\right]^2 \end{aligned}\right\} \qquad (36)$$

For the rotating disk,

$$\left.\begin{aligned} A'&=\sqrt{3}\cos\alpha+\sin\alpha\\ B'&=(\sqrt{3}\sin\alpha-\cos\alpha)\frac{1}{\tau}\frac{d\tau}{d\gamma}\\ C'&=2\cos\alpha-\sqrt{\frac{2}{3}}\rho(\omega k)^2\left(\frac{r}{k}\right)^2\frac{1}{\tau}\\ D'&=(\sqrt{3}\sin\alpha-\cos\alpha)\gamma\\ E'&=-(\sqrt{3}\cos\alpha+\sin\alpha)\\ F'&=2\sqrt{3}(\cos\alpha)\gamma \end{aligned}\right\} \qquad (37)$$

For the infinite plate with a circular hole,

$$\left.\begin{aligned} A'&=\sqrt{3}\cos\alpha+\sin\alpha\\ B'&=(\sqrt{3}\sin\alpha-\cos\alpha)\frac{1}{\tau}\frac{d\tau}{d\gamma}\\ C'&=2\cos\alpha\\ D'&=(\sqrt{3}\sin\alpha-\cos\alpha)\\ E'&=-(\sqrt{3}\cos\alpha+\sin\alpha)\\ F'&=2\sqrt{3}(\cos\alpha)\gamma \end{aligned}\right\} \qquad (38)$$

For small strains, the coefficients A', B', C', D', E', and F' are used in equation (29) instead of A, B, C, D, E, and F, respectively.

APPENDIX B

EQUATIONS FOR ROTATING DISK AND INFINITE PLATE WITH CIRCULAR HOLE IN ELASTIC RANGE

ROTATING DISK

For a solid rotating disk with the radial stress at the periphery ($r=b$) equal to zero, the principal stresses can be expressed by the following equations (reference 23, p. 68):

$$\left.\begin{aligned}\sigma_r&=\frac{3+\nu}{8}\rho\omega^2(b^2-r^2)\\ \sigma_\theta&=\frac{3+\nu}{8}\rho\omega^2b^2-\frac{1+3\nu}{8}\rho\omega^2r^2\end{aligned}\right\} \tag{39}$$

where ν is Poisson's ratio. At $r=b$,

$$(\sigma_\theta)_b=\frac{1}{4}\rho\omega^2b^2(1-\nu)$$

Dividing equation (39) by $(\sigma_\theta)_b$ yields

$$\left.\begin{aligned}\frac{\sigma_r}{(\sigma_\theta)_b}&=\frac{3+\nu}{2(1-\nu)}\left[1-\left(\frac{r}{b}\right)^2\right]\\ \frac{\sigma_\theta}{(\sigma_\theta)_b}&=\frac{3+\nu}{2(1-\nu)}\left[1-\frac{1+3\nu}{3+\nu}\left(\frac{r}{b}\right)^2\right]\end{aligned}\right\} \tag{39a}$$

The stress-strain relations of plane-stress problems in the elastic range are:

$$\left.\begin{aligned}\epsilon_r&=\frac{1}{E}(\sigma_r-\nu\sigma_\theta)\\ \epsilon_\theta&=\frac{1}{E}(\sigma_\theta-\nu\sigma_r)\end{aligned}\right\} \tag{40}$$

where E is the modulus of elasticity in tension and compression.

Substituting equations (39) into equations (40) yields:

$$\left.\begin{aligned}\epsilon_r&=\frac{1}{8E}(1-\nu)(3+\nu)(\rho\omega^2b^2)\left[1-\frac{3(1+\nu)}{3+\nu}\left(\frac{r}{b}\right)^2\right]\\ \epsilon_\theta&=\frac{1}{8E}(1-\nu)(3+\nu)(\rho\omega^2b^2)\left[1-\frac{1+\nu}{3+\nu}\left(\frac{r}{b}\right)^2\right]\end{aligned}\right\} \tag{40a}$$

or

$$\left.\begin{aligned}\frac{\epsilon_r}{(\epsilon_\theta)_b}&=\frac{3+\nu}{2}\left[1-\frac{3(1+\nu)}{3+\nu}\left(\frac{r}{b}\right)^2\right]\\ \frac{\epsilon_\theta}{(\epsilon_\theta)_b}&=\frac{3+\nu}{2}\left[1-\frac{1+\nu}{3+\nu}\left(\frac{r}{b}\right)^2\right]\end{aligned}\right\} \tag{40b}$$

The equations for the octahedral shear stress and strain given by equations (4a), (4b), and (5a) can be applied to both the elastic and the plastic ranges, but equation (5b) can be applied only in the plastic range. The octahedral shear strain in the elastic range can be calculated by equation (4b) or by using the following equation:

$$\gamma=\frac{2(1+\nu)}{E}\tau=\frac{2(1+\nu)}{E}\frac{\sqrt{2}}{3}(\sigma_r^2-\sigma_r\sigma_\theta+\sigma_\theta^2)^{1/2} \tag{41}$$

Substitute equations (39) in equation (41) to obtain:

$$\gamma=\frac{\sqrt{2}}{12E}\frac{(1+\nu)}{(3+\nu)}(\rho\omega^2b^2)$$
$$\left[(3+\nu)^2-4(1+\nu)(3+\nu)\left(\frac{r}{b}\right)^2+(7+2\nu+7\nu^2)\left(\frac{r}{b}\right)^4\right]^{1/2} \tag{41a}$$

or

$$\frac{\gamma}{\gamma_b}=\frac{1}{2(1-\nu)}$$
$$\left[(3+\nu)^2-4(1+\nu)(3+\nu)\left(\frac{r}{b}\right)^2+(7+2\nu+7\nu^2)\left(\frac{r}{b}\right)^4\right]^{1/2} \tag{41b}$$

The value of Poisson's ratio ν for the two materials are:

$\nu=0.29$ for Inconel X (reference 24)

$\nu=0.286$ for 16-25-6 (reference 25)

INFINITE PLATE WITH CIRCULAR HOLE

For a uniformly loaded infinite plate with a circular hole, the principal stresses are (reference 23, p. 56):

$$\left.\begin{aligned}\sigma_r&=\frac{A}{r^2}+2C\\ \sigma_\theta&=\frac{-A}{r^2}+2C\end{aligned}\right\} \tag{42}$$

where A and C are arbitrary constants. For the plate considered herein, the boundary conditions are:

$$\sigma_r=0 \qquad \text{at } r=a$$
$$\sigma_r=(\sigma_r)_b \quad \text{at } r=b$$

These boundary conditions are used to determine the arbitrary constants A and C, which yield

$$\left.\begin{aligned}\sigma_r&=\frac{(\sigma_r)_b}{1-\left(\frac{a}{b}\right)^2}\frac{\left(\frac{r}{a}\right)^2-1}{\left(\frac{r}{a}\right)^2}\\ \sigma_\theta&=\frac{(\sigma_r)_b}{1-\left(\frac{a}{b}\right)^2}\frac{\left(\frac{r}{a}\right)^2+1}{\left(\frac{r}{a}\right)^2}\end{aligned}\right\} \tag{42a}$$

or

$$\left.\begin{aligned}\frac{\sigma_r}{(\sigma_\theta)_b}&=\frac{1}{1+\left(\frac{a}{b}\right)^2}\frac{\left(\frac{r}{a}\right)^2-1}{\left(\frac{r}{a}\right)^2}\\ \frac{\sigma_\theta}{(\sigma_\theta)_b}&=\frac{1}{1+\left(\frac{a}{b}\right)^2}\frac{\left(\frac{r}{a}\right)^2+1}{\left(\frac{r}{a}\right)^2}\end{aligned}\right\} \tag{42b}$$

Substituting equations (42a) into equations (40) yields

$$\left.\begin{aligned}\epsilon_r&=\frac{1}{E}\frac{(\sigma_r)_b}{1-\left(\frac{a}{b}\right)^2}\frac{(1-\nu)\left(\frac{r}{a}\right)^2-(1+\nu)}{\left(\frac{r}{a}\right)^2}\\ \epsilon_\theta&=\frac{1}{E}\frac{(\sigma_r)_b}{1-\left(\frac{a}{b}\right)^2}\frac{(1-\nu)\left(\frac{r}{a}\right)^2+(1+\nu)}{\left(\frac{r}{a}\right)^2}\end{aligned}\right\} \tag{43}$$

or

$$\left.\begin{aligned}\frac{\epsilon_r}{(\epsilon_\theta)_b}&=\frac{(1-\nu)\left(\frac{r}{a}\right)^2-(1+\nu)}{\left[(1-\nu)+(1+\nu)\left(\frac{a}{b}\right)^2\right]\left(\frac{r}{a}\right)^2}\\ \frac{\epsilon_\theta}{(\epsilon_\theta)_b}&=\frac{(1-\nu)\left(\frac{r}{a}\right)^2+(1+\nu)}{\left[(1-\nu)+(1+\nu)\left(\frac{a}{b}\right)^2\right]\left(\frac{r}{a}\right)^2}\end{aligned}\right\} \tag{43a}$$

Substituting equations (42a) into equation (41) yields

$$\gamma=\frac{2\sqrt{2}(1+\nu)}{3E}\frac{(\sigma_r)_b}{1-\left(\frac{a}{b}\right)^2}\left[\frac{\left(\frac{r}{a}\right)^4+3}{\left(\frac{r}{a}\right)^4}\right]^{1/2} \tag{44}$$

or

$$\frac{\gamma}{\gamma_b}=\left\{\frac{\left(\frac{r}{a}\right)^4+3}{\left[1+3\left(\frac{a}{b}\right)^4\right]\left(\frac{r}{a}\right)^4}\right\}^{1/2}$$

REFERENCES

1. Nadai, A.: Plasticity. McGraw-Hill Book Co., Inc., 1931.
2. Nadai, A., and Donnell, L. H.: Stress Distribution in Rotating Disks of Ductile Material after the Yield Point Has Been Reached. A. S. M. E. Trans., vol. 51, pt. I, APM–51–16, 1929, pp. 173–180; discussion, pp. 180–181.
3. Gleyzal, A.: Plastic Deformation of a Circular Diaphragm under Pressure. Jour. Appl. Mech., vol. 15, no. 3, Sept. 1948, pp. 288–296.
4. Millenson, M. B., and Manson, S. S.: Determination of Stresses in Gas-Turbine Disks Subjected to Plastic Flow and Creep. NACA Rep. 906, 1948. (Formerly NACA TN 1636.)
5. MacGregor, C. W., and Tierney, W. D.: Developments in High-Speed Rotating Disk Research at M. I. T. Welding Jour. Suppl., vol. 27, no. 6, June 1948, pp. 303S–309S.
6. Holms, Arthur G., and Jenkins, Joseph E.: Effect of Strength and Ductility on Burst Characteristics of Rotating Disks. NACA TN 1667, 1948.
7. Hencky, Heinrich: Zur Theorie plastischer Deformationen und der hierdurch in Material hervorgerufenen Nachspannungen. Z. f. a. M. M., Bd. 4, Heft 4, Aug. 1924, S. 323–334.
8. Nadai, A.: Theories of Strength. A. S. M. E. Trans., vol. 55 APM–55–15, 1933, pp. 111–129.
9. Nadai, A.: Plastic Behavior of Metals in the Strain-Hardening Range. Part I. Jour. Appl. Phys., vol. 8, no. 3, March 1937, pp. 205–213.
10. Ilyushin, A. A.: Relation between the Theory of Saint Venant-Levy-Mises and the Theory of Small Elastic-Plastic Deformations. RMB–1, trans. by Appl. Math. Group, Brown Univ., for David W. Taylor Model Basin (Washington, D. C.), 1945.
11. Ilyushin, A. A.: The Theory for Small Elastic-Plastic Deformations. RMB–17, trans. by Grad. Div. Appl. Math., Brown Univ., for David W. Taylor Model Basin (Washington, D. C.), 1947. (Contract NObs–34166.)
12. Prager, W.: Strain Hardening Combined Stresses. Jour. Appl. Phys., vol. 16, no. 12, Dec. 1945, pp. 837–840.
13. Drucker, D. C.: A Reconsideration of Deformation Theories of Plasticity. A. S. M. E. Trans., vol. 71, no. 5, July 1939, pp. 587–592.
14. Davis, E. A.: Increase of Stress with Permanent Strain and Stress-Strain Relations in the Plastic State for Copper under Combined Stresses. Jour. Appl. Mech., vol. 10, no. 4, Dec. 1943, pp. A187–A196.
15. Osgood, W. R.: Combined-Stress Tests on 24S–T Aluminum Alloy Tubes. Jour. Appl. Mech., vol. 14, no. 2, June 1947, pp. A147–A153.
16. Fraenkel, S. J.: Experimental Studies of Biaxially Stressed Mild Steel in the Plastic Range. Jour. Appl. Mech., vol. 15, no. 3, Sept. 1948, pp. 193–200.
17. Davis, H. E., and Parker, E. R.: Behavior of Steel under Biaxial Stress as Determined by Tests on Tubes. Jour. Appl. Mech., vol. 15, no. 3, Sept. 1948, pp. 201–215.
18. Lankford, W. T., Low, J. R., and Gensamer, M.: The Plastic Flow of Aluminum Alloy Sheet under Combined Loads. Trans. A. I. M. E., Inst. Metals Div., vol. 171, 1947, pp. 574–604.
19. Bickley, W. G.: Formulae for Numerical Integration. The Math. Gazette, vol. XXIII, no. 256, Oct. 1939, pp. 352–359.
20. Milne, William Edmund: Numerical Calculus. Princeton Univ. Press, 1949.
21. Griffith, George E.: Experimental Investigation of the Effects of Plastic Flow in a Tension Panel with a Circular Hole. NACA TN 1705, 1948.
22. Stowell, Elbridge Z.: Stress and Strain Concentration at a Circular Hole in an Infinite Plate. NACA TN 2073, 1950.
23. Timoshenko, S.: Theory of Elasticity. McGraw-Hill Book Co., Inc., 1934.
24. Anon.: Nickel and Nickel Alloys. The International Nickel Co., Inc. (New York), 1947.
25. Fleischmann, Martin: 16–25–6 Alloy for Gas Turbines. Iron Age, vol. 157, no. 3, Jan. 17, 1946, pp. 44–53; cont., vol. 157, no. 4, Jan. 24, 1946, pp. 50–60.

U. S. GOVERNMENT PRINTING OFFICE: 1951